Pure appl. geophys. 166 (2009) 741–776
0033–4553/09/050741–36
DOI 10.1007/s00024-009-0494-1

Pure and Applied Geophysics

What Does Control Earthquake Ruptures and Dynamic Faulting? A Review of Different Competing Mechanisms

ANDREA BIZZARRI

Abstract—The fault weakening occurring during an earthquake and the temporal evolution of the traction on a seismogenic fault depend on several physical mechanisms, potentially concurrent and interacting. Recent laboratory experiments and geological field observations of natural faults revealed the presence, and sometime the coexistence, of thermally activated processes (such as thermal pressurization of pore fluids, melting of gouge and rocks, material property changes, thermally-induced chemical environment evolution), elasto-dynamic lubrication, porosity and permeability evolution, gouge fragmentation and wear, etc. In this paper, by reviewing in a unifying sketch all possible chemico–physical mechanisms that can affect the traction evolution, we suggest how they can be incorporated in a realistic fault governing equation. We will also show that simplified theoretical models that idealistically neglect these phenomena appear to be inadequate to describe as realistically as possible the details of breakdown process (i.e., the stress release) and the consequent high frequency seismic wave radiation. Quantitative estimates show that in most cases the incorporation of such nonlinear phenomena has significant, often dramatic, effects on the fault weakening and on the dynamic rupture propagation. The range of variability of the value of some parameters, the uncertainties in the relative weight of the various competing mechanisms, and the difference in their characteristic length and time scales sometime indicate that the formulation of a realistic governing law still requires joint efforts from theoretical models, laboratory experiments and field observations.

Key words: Rheology and friction of the fault zones, constitutive laws, mechanics of faulting, earthquake dynamics, computational seismology.

1. *Introduction*

Contrary to other ambits of physics, seismology presently lacks knowledge of *exact* physical law which governs natural faults and makes the understanding of earthquakes feasible from a deterministic point of view. In addition to the ubiquitous ignorance of the initial conditions (i.e., the initial state) of the seismogenic region of interest, we also ignore the equations that control the traction evolution on the fault surface; this has been recently recognized as one of the grand challenges for seismology (http://www.iris.edu/hq/lrsps/seis_lrp_12_08_08.pdf, December 2008). Indirect information comes from theoretical and numerical studies, which, under some assumptions and hypotheses, try to reproduce real–world events and aim to infer some constraints from a systematic

Istituto Nazionale di Geofisica e Vulcanologia, Sezione di Bologna, Italy. E-mail: bizzarri@bo.ingv.it

comparison of synthetics with observations. Much information arises from laboratory experiments, which, on the other hand, suffer from the technical impossibility of reproducing (in terms of confining stress *and* sliding velocity) the conditions typical of a fault during its coseismic failure. Finally, recent observations of mature faults (drilling projects and field studies) open new frontiers on the structure of faults and their composition, although at the same time they raise questions regarding physical processes occurring during faulting.

It has been widely established that earthquakes are complex at all scales, both in the distributions of slip and of stress drop on the fault surface. After the pioneering studies by Das and Aki (1977a), Aki (1979) and Day (1982), the first attempts to model complexities were the "asperity" model of Kanamori and Stewart (1976) and the "barrier" model proposed by Das and Aki (1977b). Subsequently, in his seminal paper, Madariaga (1979) showed that the seismic radiation from these models would be very complex and, more recently, Bak *et al.* (1987) suggested that complexity must be due to the spontaneous organization of a fault that is close to criticality. The slip complexity on a fault may arise from many different factors. Just for an example: (*i*) effects of heterogeneous initial stress field (Mai and Beroza, 2002; Bizzarri and Spudich, 2008 among many others); (*ii*) interactions with other active faults (Steacy *et al.*, 2005 and references therein; Bizzarri and Belardinelli, 2008); (*iii*) geometrical complexity, non–planarity, fault segmentation and branching (Poliakov *et al.*, 2002; Kame *et al.*, 2003; Fliss *et al.*, 2005; Bhat *et al.*, 2007); and (*iv*) different and competing physical mechanisms occurring within the cosesimic temporal scale, such as thermal pressurization, rock melting, mechanical lubrication, ductile compaction of gouge, inelastic deformations, etc.

In this paper we will focus on the latter aspect, which has been the object of increasing interest in recent years. Starting from the key question raised by Scholz and Hanks (2004), it is now clear that in the tribological community, as well as in the dynamic modelling community, "the central issue is whether faults obey simple friction laws, and if so, what is the friction coefficient associated with fault slip" (see also Bizzarri and Cocco, 2006d and references therein). We will discuss in the progression of the paper how these phenomena can be incorporated in a governing equation and in most cases we will show the significant effect on rupture propagation of such an inclusion.

As an opposite of a fracture criterion — which is a condition that specifies in terms of energy (Parton and Morozov, 1974) or maximum frictional resistance (Reid, 1910; Benioff, 1951) whether there is a rupture at a given fault point and time on a fault — a governing (or constitutive) law is an analytical relation between the components of stress tensor and some physical observables. Following the Amonton' s Law and the Coulomb–Navier criterion, we can relate the magnitude τ of the shear traction **T** to the effective normal stress on the fault σ_n^{eff} through the well known relation:

$$\tau = \|\mathrm{T}\| = \mu\sigma_n^{eff}, \tag{1}$$

μ being the (internal) friction coefficient and

$$\sigma_n^{eff} = \sigma_n - p_{fluid}^{wf} \tag{2}$$

(TERZAGHI *et al.*, 1996). In equation (1) an additional term for the cohesive strength C_0 of the contact surface can also appear on the right–hand side (C_0 = 1–10 MPa; RANALLI, 1995);

Table 1

List of main symbols used in the paper

Symbol	Meaning
$\tau = \|\mathrm{T}\|$	Fault traction, equations (1) and (37)
τ_{ac}	Average local shear strength of asperities contacts, equation (16)
μ	Friction coefficient
σ_n^{eff}	Effective normal stress, equations (2) and (32)
σ_n	(Reference) normal stress of tectonic origin
p_{fluid}^{wf}	Pore fluid pressure on the fault (i.e., in the middle of the slipping zone); see also equation (13) for the solution of the thermal pressurization problem
$p_{fluid}^{(lub)}$	Lubrication fluid pressure, equation (30)
$P^{(lub)}$	Approximated expression for lubrication fluid pressure, equations (32) and (36)
u	Modulus of fault slip
u_{tot}	Total cumulative fault slip
v	Modulus of fault slip velocity
Ψ	Scalar state variable for rate– and state–dependent governing laws, equation (39)
$2w$	Slipping zone thickness; see also equations (28), (29), (33) and (34)
T	Temperature field
T^{wf}	Temperature on the fault (i.e., in the center of the slipping zone), equation (8)
T_{weak}	Absolute weakening temperature of asperity contacts
κ	Thermal conductivity
ρ_{bulk}	Cubic mass density of the bulk composite
$\mathcal{C}_{bulk_p}$	Specific heat of the bulk composite at constant pressure
$\chi = \kappa/\rho_{bulk}\mathcal{C}_{bulk_p}$	Thermal diffusivity
$c \equiv \rho_{bulk}\mathcal{C}_{bulk_p}$	Heat capacity for unit volume of the bulk composite
α_{fluid}	Volumetric thermal expansion coefficient of the fluid
β_{fluid}	Coefficient of the compressibility of the fluid
ω	Hydraulic diffusivity, equation (10)
k	Permeability
η_{fluid}	Fluid viscosity; see also equation (19)
Φ	Porosity, see also equations (21) to (25)
A_{ac}	Asperity (i.e., real) contacts area
A_m	Macroscopic (i.e., nominal) area in contact
D_{ac}	Average diameter of asperity contacts
E_a	Activation energy, equations (19) and (39)
V_a	Activation volume, equation (40)
R	Universal gas constant, equations (19) and (39)
k_B	Boltzmann constant, equation (40)
h	Material hardness, equation (40)

in equation (2) σ_n is the normal stress (having tectonic origin) and p_{fluid}^{wf} is the pore fluid pressure on the fault. For convenience, we list in Table 1 the main symbols used in this paper.

Once the boundary conditions (initial conditions, geometrical settings and material properties) are specified, the value of fault friction τ controls the metastable rupture nucleation, the further (spontaneous) propagation (accompanied by stress release, seismic wave excitation and stress redistribution in the surrounding medium), the healing of slip and finally the arrest of the rupture (i.e., the termination of the seismogenic phase of the rupture), which precedes the restrengthening interseismic stage. With the only exception of slow nucleation and restrengthening, all the above–mentioned phases of the rupture process are accounted for in fully dynamic models of an earthquake, provided that the exact analytical form of the fault strength is given. The inclusion of all the previously–mentioned physical processes that can potentially occur during faulting is a clear requisite of a realistic fault governing law. In the light of this, equation (1) can be rewritten in a more verbose form as follows (generalizing equation (3.2) in BIZZARRI and COCCO, 2005):

$$\tau = \tau(w_1 O_1, w_2 O_2, \ldots, w_N O_N) \tag{3}$$

where $\{O_i\}_{i\,=\,1,\ldots,N}$ are the physical observables, such as cumulative fault slip (u), slip velocity modulus (v), internal variables (such as state variables, $\boldsymbol{\Psi}$; RUINA, 1983), etc. (see BIZZARRI and COCCO, 2005 for further details). Each observable can be associated with its evolution equation, which is coupled to equation (3).

It is unequivocal that the *relative* importance of each process (represented by the weights $\{w_i\}_{i\,=\,1,\ldots,N}$) can change depending on the specific event we consider; it is therefore very easily expected that not all independent variables O_i will appear in the expression of fault friction for all natural faults. Moreover, each phenomenon is associated with its own characteristic scale length and duration and is controlled by certain parameters, some of which are sometimes poorly constrained by observational evidence. The difference in the length (and time) scale parameters of each chemico–physical process potentially represents a theoretical complication in the effort to include different mechanisms in the governing law, as we will discuss in the following of the paper.

2. *The Fault Structure*

In Figure 1 there is a sketch representing the most widely accepted model of a fault, which is considered in the present paper. It is essentially based on the data arising from numerous field observations and geological evidence (EVANS and CHESTER, 1995; CHESTER and CHESTER, 1998; LOCKNER *et al*., 2000; HEERMANCE *et al*., 2003; SIBSON, 2003; BILLI and STORTI, 2004). Many recent investigations focussing on the internal structure of fault zones reveal that coseismic slip on mature fault often occurs within an ultracataclastic, gouge–rich and possibly clayey zone (the foliated fault core), generally having a thickness of the order of a few centimeters (2–3 mm in small faults with 10 cm of slip in

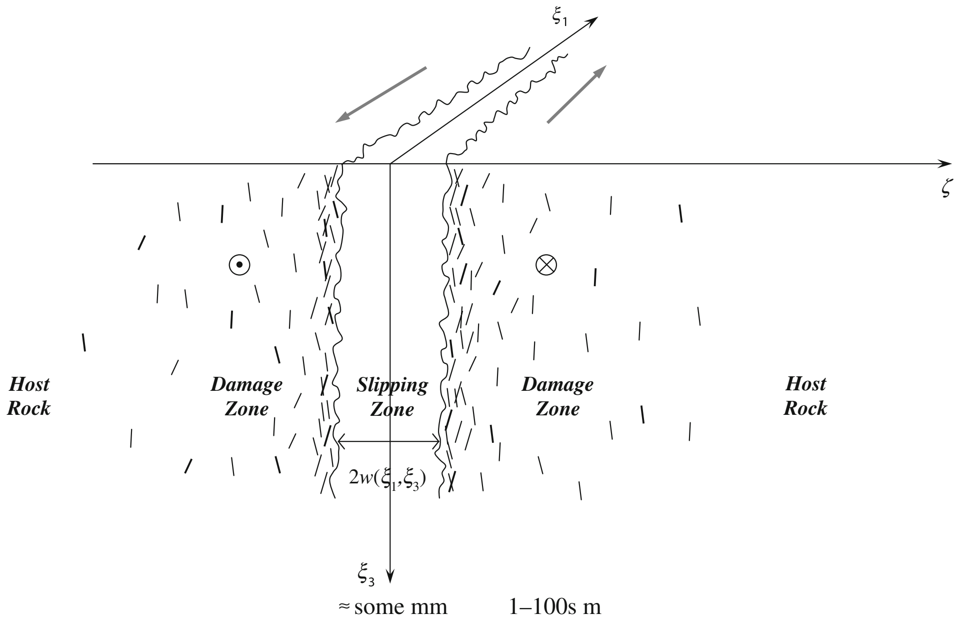

Figure 1
Sketch representing the fault structure described in section 2, as suggested by geological observations (e.g., CHESTER and CHESTER, 1998; LOCKNER *et al.*, 2000; SIBSON, 2003). The slipping zone of thickness $2w$ is surrounded by highly fractured damage zone and finally by the host rocks.

the Sierra Nevada; 10–20 cm in the Punchbowl fault). The fault core, which typically is parallel to the macroscopic slip vector, is surrounded, with an abrupt transition (CHESTER *et al.*, 2004), by a cataclastic damage zone, which can extend up to hundreds of meters. This is composed of highly fractured, brecciated and possibly granulated materials and it is generally assumed to be fluid–saturated. The degree of damage diminishes to the extent as we move far from the ultracataclastic fault core. Outside the damage zone is the host rock, composed of undamaged materials (e.g., WILSON *et al.*, 2003).

The above–mentioned observations (see also BEN–ZION and SAMMIS, 2003; CASHMAN *et al.*, 2007) tend to suggest that slip is accommodated along a single, nearly planar surface, the prominent slip surface (pss) — sometimes called principal fracture surface (pfs) — which generally has a thickness of the order of millimeters. TCHALENKO (1970) described in detail the evolution, for increasing displacement, of localized Riedel zones and conjugate set of Riedel shears, existing around the yield stress, into a concentration of rotated Riedel, P and Y shear zones within a relatively narrow and contiguous tabular zone. When the breakdown process is realized (i.e., the traction is degraded down to its kinetic, or residual, level), the fault structure reaches a mature stage and the slip is concentrated in one (or sometime two) pss, which can be in the middle or near one border of the fault core (symmetric or asymmetric disposition, respectively; see

Sibson, 2003). Moreover, field observations from exhumed faults indicate that fault zones grow in width by continued slip and evolve internally as a consequence of grains size reduction (e.g., Engelder, 1974). We will discuss a possible way to incorporate such a variation in a numerical model of earthquake rupture in section 5. As we will see in the advancement of the paper, the fault zone width, which is a key parameter for many phenomena described in this paper, is difficult to quantify even for a single fault (Rathbun and Marone, 2009) and exhibits an extreme variation along the strike direction. In extreme cases where damage is created off–fault (as in the laboratory experiments of Hirose and Bystricky, 2007) and the definition itself of the fault zone width is not straightforward. One possible (conservative) approach is to assume that the fault zone width is spatially uniform and temporally constant (see next sections 3.1 and 3.2) and to test the effects on the numerical results of the different widths, exploring the range of variability suggested by natural observations. In this way we can take into account physical constraints and, at the same time, we could try to address new laboratory experiments in order to validate the accuracy of theoretical and numerical approaches.

3. *Thermal Effects*

3.1. Temperature Changes

In this section we will focus on the thermally–activated processes. It is well known that when contacting surfaces move relative to each other the friction existing between the two objects converts kinetic energy into thermal energy, or heat. Indicating with q the rate of frictional heat generation ($[q] = \mathrm{W/m^3}$) and neglecting state changes, the temperature in a point of a thermally isotropic medium is the solution of the heat conduction equation

$$\frac{\partial}{\partial t}T = \chi\left(\frac{\partial^2}{\partial \xi_1^2} + \frac{\partial^2}{\partial \zeta^2} + \frac{\partial^2}{\partial \xi_3^2}\right)T + \frac{1}{c}q, \tag{4}$$

where (ξ_1, ξ_3) is a fault point, ζ denotes the spatial coordinate normal to the fault (see Fig. 1), χ is the thermal diffusivity ($\chi = \kappa/\rho_{bulk}\mathcal{C}_{bulk_p}$, where κ is the thermal conductivity, ρ_{bulk} is the cubic mass density of the bulk composite and $\mathcal{C}_{bulk_p}$ is the specific heat of the bulk composite at constant pressure) and $c \equiv \rho_{bulk}\mathcal{C}_{bulk_p}$ is the heat capacity for unit volume of the bulk composite. Following Bizzarri and Cocco (2006a; the reader can refer to that paper for a comprehensive discussion concerning numerical values of the parameters appearing in the model), considering that in the coseismic temporal scale the 1–D (normal to fault plane) approximation of the thermal conduction problem is acceptable and that the temperature in a fault point mainly depends on the fault slip velocity and traction time histories in that point, we have:

$$T^w(\xi_1,\zeta,\xi_3,t) = T_0 + \int_0^t \mathrm{d}t' \int_{-\infty}^{+\infty} \mathrm{d}\zeta' q(\xi_1,\zeta',\xi_3,t') K_\chi(\xi_1,\zeta-\zeta',\xi_3,t-t') \tag{5}$$

where $T_0 \equiv T(\xi_1, \zeta, \xi_3, 0)$, i.e., the host rock temperature prior to faulting, and K_χ is the Green's kernel of the conduction equation (expressed by equation (A1), with $h = 1$, of Bizzarri and Cocco, 2006a).

We can express q considering that the rate of frictional heat generation within the slipping zone (see Fig. 1) can be written as the product of the shear stress τ and the shear strain rate. According to Cardwell *et al.* (1978), Fialko (2004) and Bizzarri and Cocco (2004, 2006a, 2006b), we assume here that the shear strain rate is constant within the slipping zone. In laboratory experiments Mair and Marone (2000) have shown that this hypothesis might be adequate, but we want to remark that, in general, the slip velocity profile may be nonlinear across the slipping zone. It follows that the shear strain rate becomes the ratio of the total slip velocity v over the thickness of the slipping zone $2w$. Referring to section 2, as a first approximation of the reality we can regard $2w$ indifferently as the width of the fault core (which includes the pss), the ultracataclastic shear zone or the gouge layer. At the present state of the art we do not have a sufficiently accurate mathematical model to distinguish between these structures which are identified basically from a microstructural point of view. Therefore we will refer to $2w$ as the thickness of the slipping zone and of the gouge layer. Assuming that all the work spent to allow the fault sliding is converted into heat (Pittarello *et al.*, 2008), we can write the quantity q in equation (4) as (Bizzarri and Cocco, 2004, 2006a):

$$q(\xi_1,\zeta,\xi_3,t) = \begin{cases} \dfrac{\tau(\xi_1,\xi_3,t)\upsilon(\xi_1,\xi_3,t)}{2w(\xi_1,\xi_3)}, & t > 0, |\zeta| \le w(\xi_1,\xi_3) \\ 0, & |\zeta| > w(\xi_1,\xi_3) \end{cases} \tag{6}$$

where $2w$ explicitly depends on the on–fault coordinates; indeed, there is experimental evidence (e.g., Klinger *et al.*, 2005) that the slipping zone thickness can change along strike and dip, even on a single fault. In section 5 we also will discuss possible temporal changes of $2w$. By using (6), equation (5) can be solved analytically (Bizzarri and Cocco, 2004, 2006a, c; see also Cardwell *et al.*, 1978; Fialko, 2004):

$$T^w(\xi_1,\zeta,\xi_3,t) = T_0 + \frac{1}{4cw(\xi_1,\xi_3)} \int_0^{t-\varepsilon} \mathrm{d}t' \left\{ \mathrm{erf}\left(\frac{\zeta + w(\xi_1,\xi_3)}{2\sqrt{\chi(t-t')}}\right) - \mathrm{erf}\left(\frac{\zeta - w(\xi_1,\xi_3)}{2\sqrt{\chi(t-t')}}\right) \right\} \times \tau(\xi_1,\xi_3,t')\upsilon(\xi_1,\xi_3,t') \tag{7}$$

erf(.) being the error function $\left(\mathrm{erf}(z) \underset{\mathrm{df}}{=} \frac{2}{\sqrt{\pi}} \int_0^z e^{-x^2} \mathrm{d}x\right)$ and ε an arbitrarily small, positive, real number (see Bizzarri and Cocco, 2006a for technical details). It is clear from equation (7) that temperature changes involve the damage zone as well as the slipping zone. In the center of the slipping zone (namely in $\zeta = 0$, which can be regarded as the idealized (or virtual mathematical) fault plane), equation (7) reduces to:

$$T^{w^f}(\xi_1, \xi_3, t) = T_0^f + \frac{1}{2cw(\xi_1, \xi_3)} \int_0^{t-\varepsilon} dt' \, \mathrm{erf}\left(\frac{w(\xi_1, \xi_3)}{2\sqrt{\chi(t-t')}}\right) \tau(\xi_1, \xi_3, t') \upsilon(\xi_1, \xi_3, t') \quad (8)$$

T_0^f being the initial temperature distribution on the fault plane (i.e., $T_0^f \equiv T(\xi_1, 0, \xi_3, 0)$). Examples of temperature rises due to frictional heat are shown for different values of the slipping zone thickness in Figure 2. For a typical earthquake event, if the thickness of the slipping zone is extremely thin ($w \leq 1$ mm), the increase of temperature is significant: for a half meter of slip, and for a slipping zone 1 mm thick, the temperature change might be of the order of 800°C (Fialko, 2004; Bizzarri and Cocco, 2006a,b) and can still be sufficiently large to generate melting of gouge materials and rocks. We will discuss this issue in section 3.4.

3.2. Thermal Pressurization of Pore Fluids

The role of fluids and pore pressure relaxation on the mechanics of earthquakes and faulting is the subject of an increasing number of studies, based on a new generation of laboratory experiments, field observations and theoretical models. The interest is motivated by the fact that fluids play an important role in fault mechanics: They can affect the earthquake nucleation and earthquake occurrence (e.g., Sibson, 1986; Antonioli *et al.*, 2006), can trigger aftershocks (Nur and Booker, 1972; Miller *et al.*, 1996; Shapiro *et al.*, 2003 among many others) and can control the breakdown process through the so–called thermal pressurization phenomenon (Sibson, 1973; Lachenbruch, 1980; Mase and Smith, 1985, 1987; Kanamori and Heaton, 2000; Andrews, 2002; Bizzarri and Cocco, 2004, 2006a, b; Rice, 2006). In this paper we will focus on the coseismic time scale, however we want to remark that pore pressure can also change during the interseismic period, due to compaction and sealing of fault zones (Blanpied *et al.*, 1995; Sleep and Blanpied, 1992).

Temperature variations caused by frictional heating (equation (7) or (8)) heat both rock matrix and pore fluids; thermal expansion of fluids is paramount, since thermal expansion coefficient of water is greater than that of rocks. The stiffness of the rock matrix works against fluid expansion, causing its pressurization. Several *in situ* and laboratory observations (Lockner *et al.*, 2000) show that there is a large contrast in permeability (k) between the slipping zone and the damage zone: in the damage zone k might be three orders of magnitude greater than that in the fault core (see also Rice, 2006). Consequently, fluids tend to flow in the direction perpendicular to the fault. Pore pressure changes are associated to temperature variations caused by frictional heating, temporal changes in porosity and fluid transport through the equation:

$$\frac{\partial}{\partial t} p_{fluid} = \frac{\alpha_{fluid}}{\beta_{fluid}} \frac{\partial}{\partial t} T - \frac{1}{\beta_{fluid} \Phi} \frac{\partial}{\partial t} \Phi + \omega \frac{\partial^2}{\partial \zeta^2} p_{fluid} \quad (9)$$

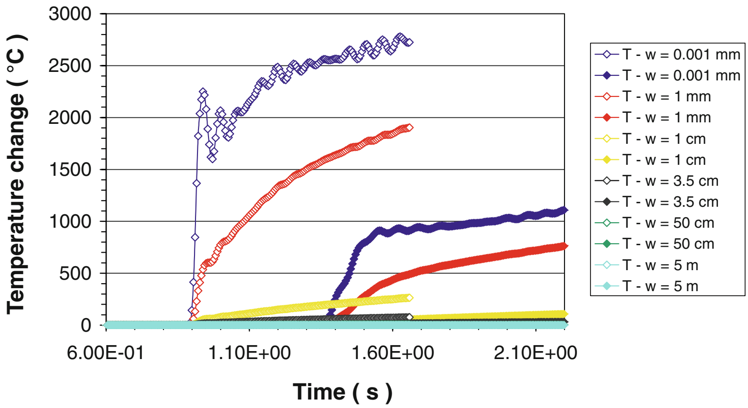

Figure 2
Temperature rises w. r. to $T_0^f = 100°\mathrm{C}$ for different values of the slipping zone thickness $2w$ on a vertical strike-slip fault obeying the linear slip–weakening law (IDA, 1972). Temperatures time histories are calculated from equation (8) at the hypocentral depth (6200 m) and at a distance along the strike of 2750 m from the hypocenter. Solid symbols refer to a configuration with strength parameter $S = 1.5$; empty ones are for $S = 0.8$. From BIZZARRI and COCCO (2006a).

where α_{fluid} is the volumetric thermal expansion coefficient of the fluid, β_{fluid} is the coefficient of the compressibility of the fluid and ω is the hydraulic diffusivity, expressed as (e.g., WIBBERLEY, 2002):

$$\omega \equiv \frac{k}{\eta_{fluid}\Phi\beta_{fluid}}, \tag{10}$$

η_{fluid} being the dynamic fluid viscosity and Φ the porosity[1]. The solution of equation (9), coupled with the heat conduction equation, can be written in the form:

$$p^w_{fluid}(\xi_1,\zeta,\xi_3,t) = p_{fluid_0} + \frac{\alpha_{fluid}}{\beta_{fluid}}\int_0^t \mathrm{d}t' \int_{-\infty}^{+\infty} \mathrm{d}\zeta' \left\{\frac{q(\xi_1,\zeta',\xi_3,t')}{\omega-\chi}\cdot\right.$$
$$\left.\left(-\chi K_\chi(\xi_1,\zeta-\zeta',\xi_3,t-t') + \omega K_\omega(\xi_1,\zeta-\zeta',\xi_3,t-t')\right)\right\} \tag{11}$$

From equation (11) it emerges that there is a coupling between temperature and pore fluid pressure variations; in the case of constant diffusion coefficients, rearranging terms of equation (11), we have that $p^w_{fluid}(\xi_1,\zeta,\xi_3,t) - p_{fluid_0} = -\frac{\chi}{\omega-\chi}\frac{\alpha_{fluid}}{\beta_{fluid}}\ (T^w(\xi_1,\ \zeta,\ \xi_3,t) - T_0) + \frac{\omega}{\omega-\chi}\frac{\alpha_{fluid}}{\beta_{fluid}}\cdot \int_0^t \mathrm{d}t' \int_{-\infty}^{+\infty} \mathrm{d}\zeta' \left\{\frac{q(\xi_1,\zeta',\xi_3,t')}{\omega-\chi} K_\omega\ (\xi_1\zeta - \zeta',\xi_3,t-t')\right\}$.

[1] Equation (9) is derived under the assumption that permeability (k), dynamic density (η_{fluid}) and cubic mass density of the fluid are spatially homogeneous. The quantity $\Phi\beta_{fluid}$ in equation (10) is an adequate approximation of the storage capacity, $\beta_c = \Phi(\beta_{fluid} - \beta_{grain}) + (\beta_{bulk} - \beta_{grain})$, because the compressibilities of mineral grain (β_{grain}) and bulk composite (β_{bulk}) are negligible w. r. to β_{fluid}.

For the specific heat source in (6), equation (11) becomes (BIZZARRI and COCCO, 2006b):

$$p^{w}_{fluid}(\xi_1,\zeta,\xi_3,t) = p_{fluid_0} + \frac{\gamma}{4w(\xi_1,\xi_3)}\int_0^{t-\varepsilon} dt' \left\{ -\frac{\chi}{\omega-\chi}\left[\mathrm{erf}\left(\frac{\zeta+w(\xi_1,\xi_3)}{2\sqrt{\chi(t-t')}}\right) - \mathrm{erf}\left(\frac{\zeta-w(\xi_1,\xi_3)}{2\sqrt{\chi(t-t')}}\right)\right] + \frac{\omega}{\omega-\chi}\left[\mathrm{erf}\left(\frac{\zeta+w(\xi_1,\xi_3)}{2\sqrt{\omega(t-t')}}\right) - \mathrm{erf}\left(\frac{\zeta-w(\xi_1,\xi_3)}{2\sqrt{\omega(t-t')}}\right)\right]\right\}\left\{\tau(\xi_1,\xi_3,t')\upsilon(\xi_1,\xi_3,t'). - \frac{2w(\xi_1,\xi_3)}{\gamma}\frac{1}{\beta_{fluid}\Phi(t')}\frac{\partial}{\partial t'}\Phi(\xi_1,\zeta,\xi_3,t')\right\} \tag{12}$$

which is simplified to

$$p^{w_f}_{fluid}(\xi_1,\xi_3,t) = p^{f}_{fluid_0} + \frac{\gamma}{2w(\xi_1,\xi_3)}\int_0^{t-\varepsilon} dt' \left\{ -\frac{\chi}{\omega-\chi}\mathrm{erf}\left(\frac{w(\xi_1,\xi_3)}{2\sqrt{\chi(t-t')}}\right). + \frac{\omega}{\omega-\chi}\mathrm{erf}\left(\frac{w(\xi_1,\xi_3)}{2\sqrt{\omega(t-t')}}\right)\right\}\left\{\tau(\xi_1,\xi_3,t')\upsilon(\xi_1,\xi_3,t') - \frac{2w(\xi_1,\xi_3)}{\gamma}\frac{1}{\beta_{fluid}\Phi(t')}\frac{\partial}{\partial t'}\Phi(\xi_1,0,\xi_3,t')\right\} \tag{13}$$

in the middle of the slipping zone. In previous equations p_{fluid_0} the initial pore fluid pressure (i.e., $p_{fluid_0} \equiv p_{fluid}(\xi_1,\zeta,\xi_3,0)$) and $\gamma \equiv \alpha_{fluid}/(\beta_{fluid}c)$. In (12) and (13) the term involving Φ accounts for compaction or dilatation and it acts in competition with respect to the thermal contribution to the pore fluid pressure changes. Additionally, variations in porosity will modify, at every time instant (see equation (10)), the arguments of error functions which involve the hydraulic diffusivity.

As a consequence of equations (1) and (2), it follows from equation (13) that variations in pore fluid pressure lead to changes in fault friction. In fact, in their fully dynamic, spontaneous, *truly* 3–D (i.e., not mixed–mode as in ANDREWS, 1994) earthquake model BIZZARRI and COCCO (2006a, b) demonstrated that the inclusion of fluid flow in the coseismic process strongly alters the dry behavior of the fault, enhancing instability, even causing rupture acceleration to super–shear rupture velocities for values of strength parameter ($S \underset{\mathrm{df}}{=} \frac{\tau_u-\tau_0}{\tau_0-\tau_f}$; DAS and AKI, 1977a, b) which do not allow this transition in dry conditions (see also BIZZARRI and SPUDICH, 2008). For extremely localized slip (i.e., for small values of slipping zone thickness) or for low value of hydraulic diffusivity, the thermal pressurization of pore fluids increases the stress drop, causing a near complete stress release (see also ANDREWS, 2002), and changes the shape of the slip–weakening curve and therefore the value of the so–called fracture energy. In Figure 3 we report slip–

weakening curves obtained in the case of Dieterich–Ruina law (LINKER and DIETERICH, 1992) for different vales of $2w$, ω and α_{DL}[2]. It has been emphasized (BIZZARRI and COCCO, 2006a, b) that in some cases it is impossible to determine the equivalent slip–weakening distance (in the sense of OKUBO, 1989 and COCCO and BIZZARRI, 2002; see also TINTI *et al.*, 2004) and the friction exponentially decreases as recently suggested by several authors (ABERCROMBIE and RICE, 2005; MIZOGUCHI *et al.*, 2007 and SUZUKI and YAMASHITA, 2007).

If we are interested in considering temporal windows longer than those typical of coseismic ruptures, we emphasize that equations (7) and (12) can be directly applicable not only in a perfectly elastic model, but also in cases accounting for a more complex rheology, where stress tensor components explicitly depend on variations of temperature (ΔT) and pore fluid pressure (Δp_{fluid}) fields (e.g., BOLEY and WEINER, 1985):

$$\sigma_{ij} = 2Ge_{ij} + \lambda e_{kk}\delta_{ij} - \frac{2G+3\lambda}{3}\alpha_{soild}\Delta T\delta_{ij} - \left(1 - \frac{2G+3\lambda}{3}\beta_{soild}\right)\Delta P_{fluid}\delta_{ij} \tag{14}$$

where G is the rigidity, λ is the first Lamé' s constant, $\{e_{ij}\}$ is the deformation tensor and Einstein' s convention on repeated indices is assumed. In (14) α_{solid} is the volumetric thermal expansion coefficient of the solid phase and β_{solid} is the compressibility of the solid devoid of any cavity, expressing the pressure necessary to change its volume (i.e., the interatomic spacing). The third term on the right–hand side in equation (14) accounts for the thermal strain of an elastic body, due to thermal expansion.

We finally recognize that in the solution of the thermal pressurization problem presented above we neglected the advection of pore fluids (approximation which has been shown to be valid if permeability is lower than 10^{-16} m^2 (LACHENBRUCH, 1980; MASE and SMITH, 1987; LEE and DELANEY, 1987)). In of generality an additional term will appear in the right–hand side of equation (4), which becomes

$$\frac{\partial T}{\partial t} = \chi\frac{\partial^2 T}{\partial \zeta^2} + \frac{1}{c}q - \frac{k}{\eta_{fluid}}\frac{\partial T}{\partial \zeta}\frac{\partial p_{fluid}}{\partial \zeta} \tag{15}$$

This will add a direct coupling between temperature and pore fluid pressure, and therefore analytical solutions (7) and (12) are no longer valid.

3.3. *Flash Heating*

Another physical phenomenon associated with frictional heat is the flash heating (TULLIS and GOLDSBY, 2003; HIROSE and SHIMAMOTO, 2003; PRAKASH and YUAN, 2004; RICE, 2006; HAN *et al.*, 2007; HIROSE and BYSTRICKY, 2007) which might be invoked to explain the reduction of the friction coefficient μ from typical values at low slip rate

[2] The parameter α_{DL} controls the coupling of the pore fluid pressure and the evolution of the state variable. It typically ranges between 0.2 and 0.56 (LINKER and DIETERICH, 1992). A null value of α_{DL} means that the evolution equation for the state variable does not depend on the effective normal stress and that the pore fluid affects only the expression of the fault friction τ.

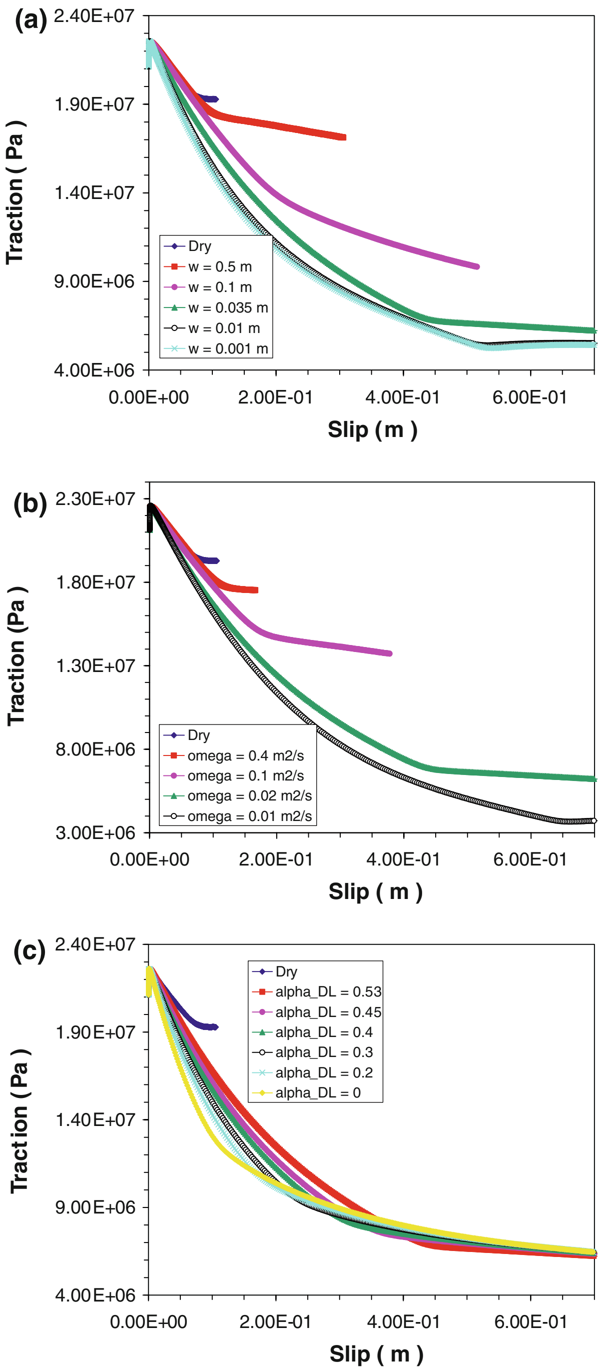

(a)
2.40E+07
1.90E+07
1.40E+07
9.00E+06
4.00E+06
Traction (Pa)
Dry
w = 0.5 m
w = 0.1 m
w = 0.035 m
w = 0.01 m
w = 0.001 m
0.00E+00
2.00E-01
4.00E-01
6.00E-01
Slip (m)
(b)
2.30E+07
1.80E+07
1.30E+07
8.00E+06
3.00E+06
Traction (Pa)
Dry
omega = 0.4 m2/s
omega = 0.1 m2/s
omega = 0.02 m2/s
omega = 0.01 m2/s
0.00E+00
2.00E-01
4.00E-01
6.00E-01
Slip (m)
(c)
2.40E+07
1.90E+07
1.40E+07
9.00E+06
4.00E+06
Traction (Pa)
Dry
alpha_DL = 0.53
alpha_DL = 0.45
alpha_DL = 0.4
alpha_DL = 0.3
alpha_DL = 0.2
alpha_DL = 0
0.00E+00
2.00E-01
4.00E-01
6.00E-01
Slip (m)

◀ Figure 3

Slip–weakening curves for a rupture governed by the LINKER and DIETERICH (1992) friction law and considering thermal pressurization of pore fluids (see section 3.2 for further details). Solutions are computed at a distance along strike of 1300 m from the hypocenter. (a) Effect of different slipping zone thickness, $2w$. (b) Effect of different hydraulic diffusivities, ω. (c) Effect of different couplings between pore fluid pressure and state variable. In all panels blue diamonds refer to a dry fault, without fluid migration. From BIZZARRI and COCCO (2006b).

($\mu = 0.6$–0.9 for most all rock types; e.g., BYERLEE, 1978) down to $\mu = 0.2$–0.3 at seismic slip rate. It is assumed that the macroscopic fault temperature (T^{wf}) changes substantially more slowly than the temperature on an asperity contact (since the asperity (i.e., real) contact area, A_{ac}, is smaller than the macroscopic (nominal) area in contact, A_m), causing the rate of heat production at the local contact to be higher than the average heating rate of the nominal area. In the model, flash heating is activated if the sliding velocity is greater than the critical velocity

$$\upsilon_{fh} = \frac{\pi\chi}{D_{ac}}\left(c\,\frac{T_{weak} + T^{wf}}{\tau_{ac}}\right)^2 \tag{16}$$

where τ_{ac} is the local shear strength of an asperity contact (which is far larger than the macroscopic applied stress; $\tau_{ac} \sim 0.1\ G =$ few GPa), D_{ac} ($\sim$few μm) its diameter and T_{weak} ($\sim$several 100 s of °C, near the melting point) is a weakening temperature at which the contact strength of an asperity begin to decrease. Using the parameters of RICE (2006) we obtain that v_{fh} is of the order of several centimeters per second; we remark that v_{fh} changes in time as does macroscopic fault temperature T^{wf}. When fault slip exceeds v_{fh} the analytical expression of the steady–state friction coefficient becomes:

$$\mu^{ss}_{fh}(\upsilon) = \mu_{fh} + \left[\mu_* - (b-a)\ln\left(\frac{\upsilon}{\upsilon_*}\right) - \mu_{fh}\right]\frac{\upsilon_{fh}}{\upsilon}, \tag{17}$$

being μ_*, μ_{fh} and v_* reference values for friction coefficient and velocity, respectively, and b and a the dimensionless constitutive parameters of the Dieterich–Ruina governing equations (DIETERICH, 1979; RUINA, 1983). For $v < v_{fh}$, on the contrary, $\mu^{ss}(v)$ retains the classical form $\left(\text{i.e., } \mu^{ss}_{lv}(\upsilon) = \left[\mu_* - (b-a)\ln\left(\frac{\upsilon}{\upsilon_*}\right)\right]\right)$.

We note that thermal pressurization of pore fluids and flash heating are inherently different mechanisms because they have a different length scale: the former is characterized by a length scale on the order of few micron (D_{ac}), while the length scale of the latter phenomenon is the thermal boundary layer ($\delta = \sqrt{2\chi t_d}$, where t_d is the duration of slip, of the order of seconds), which is $\sim$ mm up to a few cm. Moreover, while thermal pressurization affects the effective normal stress, flash heating causes changes only in the analytical expression of the friction coefficient at high slip rates. In both cases the evolution equation for the state variable is modified: by the coupling of variations in σ_n^{eff} for the first phenomenon, by the presence of additional terms involving v_{fh}/v in the latter. In a recent paper, NODA *et al.* (2009) integrate both flash heating and thermal pressurization in a single constitutive framework, as described above. Their results are properly constrained to the scale of typical laboratory experiments. When we try to apply the model to real–world events, we would encounter the well–known problem of scaling the values of the parameters of the rate– and state–dependent friction law (in whom the two phenomena are simultaneously incorporated) from laboratory–scale to real faults. This, which is particularly true for the scale distance for the evolution of the state variable, would additionally raise the problem to properly resolve, from a numerical point of view, the different spatial scales of flash heating and thermal pressurization.

3.4. Gouge and Rocks Melting

As pointed out by JEFFREYS (1942), MCKENZIE and BRUNE (1972) and FIALKO and KHAZAN (2005), melting should probably occur during coseismic slip, typically after rocks comminution. Rare field evidence for melting on exhumed faults (i.e., the apparent scarcity of glass or pseudotachylytes, natural solidified friction melts produced during coseismic slip) generates scepticism for the relevance of melt in earthquake faulting (SIBSON and TOY, 2006; REMPEL and RICE, 2006). However, several laboratory experiments have produced melt, when typical conditions of seismic deformation are attained (SPRAY, 1995; TSUTSUMI and SHIMAMOTO, 1997; HIROSE and SHIMAMOTO, 2003). Moreover, as mentioned in section 3.1, it has been demonstrated by theoretical models that for thin slipping zones (i.e., $2w/\delta < 1$) melting temperature T_m can easily be exceeded in dynamic motion (FIALKO, 2004; BIZZARRI and COCCO, 2006a, b). Even if performed at low (2–3 MPa) normal stresses, the experiments of TSUTSUMI and SHIMAMOTO (1997) demonstrated significant deviations from the predictions obtained with the usual rate– and state–friction laws (e.g., DIETERICH, 1979; RUINA, 1983). FIALKO and KHAZAN (2005) suggested that fault friction simply follows the Coulomb–Navier equation (1) before melting and the Navier–Stokes constitutive relation $\tau = \eta_{melt} \frac{v}{2w_{melt}}$ after melting ($2w_{melt}$ being the thickness of the melt layer).

NIELSEN *et al.* (2008) theoretically interpreted the results from high velocity (i.e., with $v > 0.1$ m/s) rotary friction experiments on India Gabbro and derived the following relation expressing the fault traction in steady–state conditions (i.e., when $\partial T/\partial t = 0$ in (4)) when melting occurs:

$$\tau = {\sigma_n^{eff}}^{1/4} \frac{K_{NEA}}{\sqrt{R_{NEA}}} \sqrt{\frac{\ln\left(\frac{2v}{v_m}\right)}{\frac{2v}{v_m}}} \tag{18}$$

where K_{NEA} is a dimensional normalizing factor, R_{NEA} is the radius of the contact area (i.e., the radius of sample; $R_{NEA} \approx 10 - 20$ mm in their lab experiments) and v_m is a characteristic slip rate ($v_m \leq 14$ cm/s).

3.5. *Additional Effects of Temperature*

3.5.1 Material property changes. An additional complication in the model described above can also arise from the dependence of properties of the materials on temperature. For the sake of simplicity, we neglect the variations of rigidity, volume and density of fault fluids and the surrounding medium due to temperature and pressure, even if they might be relevant[3]. We will focus our attention on the rheological properties of the fault. It is well known that the yield strength depends on temperature and that at high temperatures and pressures failure can result in ductile flow, instead that brittle failure (e.g., RANALLI, 1995). Moreover, dynamic fluid viscosity also strongly depends on temperature, through the Arrhenious Law (also adopted in cases where fluid is represented by melted silicates; see FIALKO and KHAZAN, 2005 and references therein):

$$\eta_{fluid} = K_0 e^{\frac{E_a}{RT}} \tag{19}$$

where E_a is the activation energy, R is the universal gas constant ($E_a/R \approx 3 \times 10^4$ K) and K_0 is a pre–exponential reference factor (which in some cases also might be temperature–dependent; typically is $K_0 = 1.7 \times 10^3$ Pa s for basalts and $K_0 = 2.5 \times 10^6$ Pa s for granites). This explicit dependence on the absolute temperature T will add an implicit dependence on temperature in the hydraulic diffusivity (see equation (10)), which in turn strongly affects the pore pressure evolution, as mentioned in section 3.2. As for an example, for a temperature change from 100°C to 300°C we might expect a variation in η_{fluid} of about – 83%, which in turn translates in to a dramatic change in ω (nearly 500% for typical parameters; see Table 1 in BIZZARRI and COCCO, 2006a). We note that such a continuous variation in ω can be easily incorporated in a thermal pressurization model, simply by coupling (19) with (10) and (13).

Furthermore, fluid compressibility increases with increasing temperature (WIBBERLEY, 2002) and this causes additional temporal variations in hydraulic diffusivity. Finally, also thermal conductivity changes with absolute temperature, according to the following equation:

$$\kappa = K_1 + \frac{K_2}{T + 77} \tag{20}$$

where $K_1 = 1.18$ J/(kg K) and $K_2 = 474$ J/kg (CLAUSER and HUENGES, 2000). For the parameters used in BIZZARRI and COCCO (2006a), equation (20) implies a decrease of 16%

[3] For instance, a temperature change of 200°C can lead to a variation of the order of 30% in fluid density (since $\frac{d\rho_{fluid}}{\rho_{fluid}} = -\alpha_{fluid} dT$).

in thermal diffusivity χ for a temperature rise from 100°C to 300°C and this will directly affect the evolution of the pore fluid pressure (see again equation (13)).

3.5.2 Chemical environment changes. It is known that fault friction can be influenced also by chemical environment changes. Without any clear observational evidence, OHNAKA (1996) assumed that the chemical effects of pore fluids (as that of all other physical observables), are negligible compared to that of fault slip. On the contrary, chemical analyses of gouge particles formed in high velocity laboratory experiments by HIROSE and BYSTRICKY (2007) showed that dehydration reactions (i.e., the release of structural water in serpentine) can take place. Moreover, recent experiments on Carrara marble performed by HAN *et al.* (2007) using a rotary–shear, high–velocity friction apparatus demonstrated that thermally activated decomposition of calcite (into lime and CO_2 gas) occurs from a very early stage of slip, in the same temporal scale as the ongoing and enhanced fault weakening. Thermal decomposition weakening may be a widespread chemico–physical process, since natural gouges commonly are known to contain sheet silicate minerals. The latter can decompose, even at lower temperatures than that for calcite decomposition, and can leave geological signatures of seismic slip (HAN *et al.*, 2007), different from pseudotachylytes. Presently, there are no earthquake models in which chemical effects are incorporated within a governing equation. We believe that efforts will be directed to this goal in the near future.

4. *Porosity and Permeability Changes*

4.1. *Porosity evolution*

As pointed out by BIZZARRI and COCCO (2006a, b), values of permeability (k), porosity (Φ) and hydraulic diffusivity (ω) play a fundamental role in controlling the fluid migration and the breakdown processes on a seismogenic fault. During an earthquake event frictional sliding tends to open (or dilate) cracks and pore spaces (leading to a decrease in pore fluid pressure), while normal traction tends to close (or compact) cracks (therefore leading to a pore fluid pressure increase). Stress readjustment on the fault can also switch from ineffective porosity (i.e., closed, or non–connected, pores) to effective porosity (i.e., catenary pores), or *vice versa*. Both ductile compaction and frictional dilatancy cause changes to k, Φ and therefore to ω. It is clear from equation (13) that this leads to variations to p_{fluid}^{wf}.

Starting from the theory of ductile compaction of MCKENZIE (1984) and assuming that the production rate of the failure cracks is proportional to the frictional strain rate and combining the effects of the ductile compaction, SLEEP (1997) introduced the following evolution equation for the porosity:

$$\frac{\mathrm{d}}{\mathrm{d}t}\phi = \frac{\upsilon\beta_{cp}\mu_*}{2w} - \frac{\sigma_n^{eff^n}}{C_\eta(\phi_{sat}-\phi)^m} \tag{21}$$

where β_{cp} is a dimensionless factor, C_η is a viscosity parameter with proper dimensions, n is the creep power law exponent and m is an exponent that includes effects of nonlinear rheology and percolation theory[4]. Equation (21) implies that porosity cannot exceed a saturation value ϕ_{sat}.

As noted by SLEEP and BLANPIED (1992), frictional dilatancy also is associated with the formation of new voids, as well as with the intact rock fracturing (i.e., with the formation of new tensile microcracks; see VERMILYE and SCHOLZ, 1988). In fact, it is widely accepted (e.g., OHNAKA, 2003) that earthquakes result in a complex mixture of frictional slip processes on pre–existing fault surfaces and shear fracture of initially intact rocks. This fracturing will cause a change in porosity; fluid within the fault zone drains into these created new open voids and consequently decreases the fluid pressure. The evolution law for the porosity associated with the new voids is (SLEEP, 1995):

$$\frac{\mathrm{d}}{\mathrm{d}t}\phi = \frac{\upsilon\beta_{ov}\mu}{2w}, \tag{22}$$

where the factor β_{ov} is the fraction of energy that creates the new open voids[5].

SLEEP (1997) also proposed the following relation that links the increase of porosity to the displacement: $\frac{\partial}{\partial u}\Phi = \frac{\Phi\alpha_{fluid}\tau}{2wc}$. This leads to an evolution law for porosity:

$$\frac{\mathrm{d}}{\mathrm{d}t}\Phi = \frac{\Phi\alpha_{fluid}\tau}{2wc} \tag{23}$$

Finally, SEGALL and RICE (1995) proposed two alternative relations for the evolution of Φ. The first mimics the evolution law for state variable in the Dieterich–Ruina model (BEELER *et al.*, 1994 and references therein):

$$\frac{d}{dt}\Phi(\xi_1,\zeta,\xi_3,t) = -\frac{\upsilon}{L_{SR}}\left[\Phi(\xi_1,\zeta,\xi_3,t) - \varepsilon_{SR}\ln\left(\frac{c_1\upsilon + c_2}{c_3\upsilon + 1}\right)\right], \tag{24}$$

where ε_{SR} ($\varepsilon_{SR} < 3.5 \times 10^{-4}$ from extrapolation to natural fault of SEGALL and RICE, 1995) and L_{SR} are two parameters representing the sensitivity to the state variable evolution (in the framework of rate– and state–dependent friction laws) and a characteristic length–scale, respectively, and $\{c_i\}_{i=1,2,3}$ are constants ensuring that Φ is in the range [0,1]. In principle, ε_{SR} can decrease with increasing effective normal stress, although present by we have no detailed information about this second–order effect.

The second model, following SLEEP (1995), postulates that Φ is an explicit function on the state variable Ψ:

[4] The exponent m in equation (19) can be approximated as (KRAJCINOVIC, 1993): $m \cong 2 + 0.85(n+1)$.

[5] It is important to remark that in (22) an absolute variation of the porosity is involved, while in (21) a relative change is involved.

$$\Phi(\xi_1, \zeta, \xi_3, t) = \Phi_* - \varepsilon_{SR} \ln\left(\frac{\Psi v_*}{L_{SR}}\right). \tag{25}$$

Φ_* being a reference value, assumed to be homogeneous over the entire slipping zone thickness. Considering the latter equation, coupled with (13), and assuming as SEGALL and RICE (1995) that the scale lengths for the evolution of porosity and state variable are the same, BIZZARRI and COCCO (2006b) showed that even if the rupture shape, the dynamic stress drop and the final value of σ_n^{eff} remain unchanged w. r. to a corresponding simulated event in which a constant porosity was assumed, the weakening rate is not constant for increasing cumulative slip. Moreover, they showed that the equivalent slip–weakening distance becomes meaningless. This is clearly visible in Figure 4, where we compare the solutions of the thermal pressurization problem in cases of constant (black curve) and variable porosity (gray curve).

All the equations presented in this section clearly state that porosity evolution is concurrent with the breakdown processes, since it follows the evolution of principal variables involved in the problem (v, τ, σ_n^{eff}, Ψ). However, in spite of the above–mentioned profusion of analytical relations (see also SLEEP, 1999), porosity is one of the biggest unknowns in the fault structure and presently available evidence from the laboratory, and from geological observations as well, does not allow us to discriminate between different possibilities. Only numerical experiments performed by coupling one of the equations (21) to (25) with (13) can show the effects of different assumptions and suggest what is the most appropriate. Quantitative results will be reported at a later date and they will plausibly give useful indications for the design of laboratory experiments.

4.2. Permeability Changes

As mentioned above, changes in hydraulic diffusivity can be due not only to the time evolution of porosity, but also to variations of permeability. k is known to suffer large variations with type of rocks and their thermo–dynamical state (see for instance TURCOTTE and SCHUBERT, 1982) and moreover local variation of k has been inferred near the fault (JOURDE *et al.*, 2002). Several laboratory results (BRACE *et al.*, 1968; PRATT *et al.*, 1977; BRACE, 1978; HUENGES and WILL, 1989) supported the idea that k is an explicit function of σ_n^{eff}. A reasonable relation (RICE, 1992) is:

$$k = k_0 e^{-\frac{\sigma_n^{eff}}{\sigma_*}}, \tag{26}$$

where k_0 is the permeability at zero effective normal stress and σ_* is a constant (between 5 and 40 MPa). For rocks in the center of the Median Tectonic Line fault zone (Japan) WIBBERLEY and SHIMAMOTO (2005; their Figure 2a) found the same relation with $k_0 = 8.71 \times 10^{-21}$ m^2 and $\sigma_* = 30.67$ MPa. For typical changes in σ_n^{eff} expected during coseismic ruptures (see for instance Figures 3c and 5d of BIZZARRI and COCCO, 2006a) we can estimate an increase in k at least of a factor 2 within the temporal scale of the

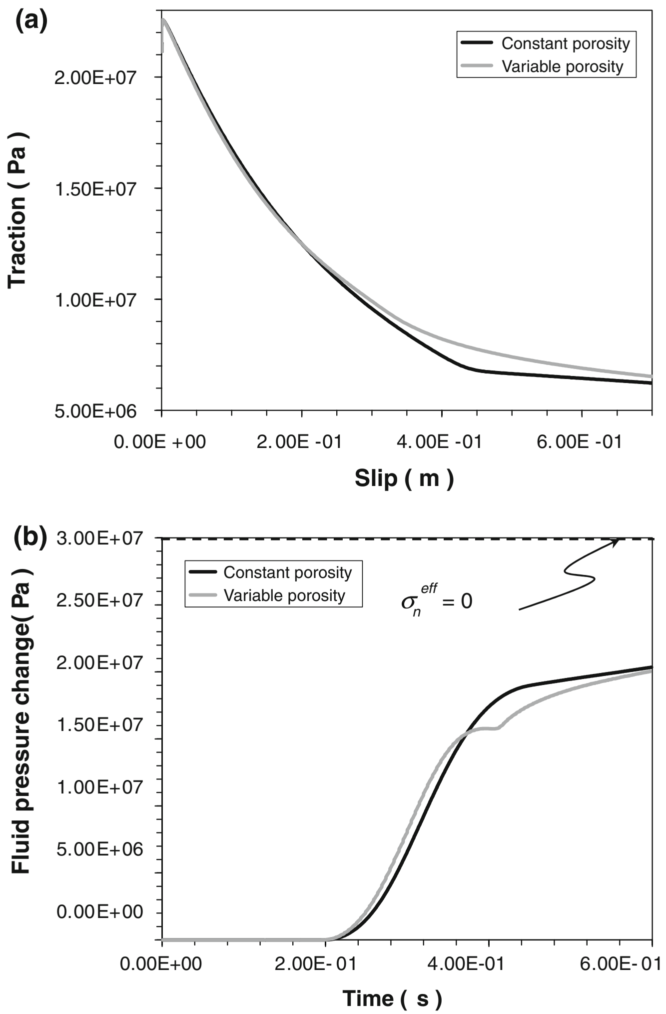

Figure 4

Comparison between solutions of the thermal pressurization problem in the case of constant (black curve) and variable porosity (as described by equation (25); gray curve). (a) Traction vs. slip curve, emphasizing that the equivalent slip–weakening distance becomes meaningless in the case of variable porosity. (b) Traction evolution of the effective normal stress. The relative minimum in σ_n^{eff} is the result of the competition between the two terms in equation (13), the thermal contribution and the porosity contribution. From Bizzarri and Cocco (2006b).

dynamic rupture. In principle, this can counterbalance the enhancement of instability due to the fluid migration out of the fault. This is particularly encouraging because seismological estimates of the stress release (almost ranging from about 1 to 10 MPa; Aki, 1972; Hanks, 1977) do not support the evidence of a nearly complete stress drop, as predicted by numerical experiments of thermal pressurization (Andrews, 2002; Bizzarri and Cocco, 2006a, b).

Another complication may arise from the explicit dependence of permeability on porosity and on grain size d. Following one of the most widely accepted relation, the Kozeny–Carman equation (Kozeny, 1927; Carman, 1937, 1956), we have:

$$k = K_{KC} \frac{\Phi^3}{1 - \Phi^2} d^2, \tag{27}$$

where $K_{KC} = 8.3 \times 10^{-3}$. Gouge particle refinement and temporal changes in Φ, such as that described in equations (21) to (25), affect the value of k.

As in the case of porosity evolution, permeability changes also occur during coseismic fault traction evolution and equations (26) or (27) can be easily incorporated in the thermal pressurization model (i.e., coupled with equation (12)).

5. *Gouge evolution and Gelation*

Numerous number of laboratory and geological studies on mature faults (among the others Tullis and Weeks, 1986) emphasized that, during sliding, a finite amount of wear is progressively generated by abrasion, fragmentation and pulverization of rocks (see also Sammis and Ben–Zion, 2007). Further slip causes comminution (or refinement) of existing gouge particles, leading to a net grain size reduction and finally to the slip localization onto discrete surface (see also section 2). There is also evidence that the instability of natural faults is controlled by the presence of granular wear products (see for instance Marone *et al.*, 1990). Power *et al.* (1988) suggested that natural rock surface roughness leads to a linear relationship between wear zone width and cumulative slip:

$$2w \cong 2K_{PEA} u \tag{28}$$

($K_{PEA} = 0.01$[6]), which in principle complicates the solution of the thermal pressurization problem, because it will insert an implicit temporal dependence in the slipping zone thickness. Temporal variations of $2w$ are also expected as a consequence of thermal erosion of the host rocks (e.g., Jeffreys, 1942; McKenzie and Brune, 1972). More plausibly, in natural faults the variations in $2w$ described by equation (28) are appreciable if we consider the entire fault history, and not within the coseismic temporal scale. In equation (28) u has therefore to be regarded as the total fault slip after each earthquake event (u_{tot_n}); in light of this, equation (28) is in agreement with the empirical relation found by Scholz (1987). The increasing value of this cumulative slip leads to a net increase in $2w$ and this further complicates the constraints on this important parameter.

Inversely, Marone and Kilgore (1993) and Mair and Marone (1999) experimentally found that

[6] This value agrees with Robertson (1983).

$$\frac{\Delta w}{\Delta Log(v_{load})} = K_{MK}, \tag{29}$$

where v_{load} is the loading velocity in the laboratory apparatus and K_{MK} is a constant depending on the applied normal stress. As an example, a step in v_{load} from 1 to 10 mm/s will raise $2w$ by 8 μm at $\sigma_n = 25$ MPa. Unfortunately, the extrapolation to natural fault conditions is not trivial.

Another interesting and non–thermal mechanism related to the gouge particle comminution is the silica gel formation (GOLDSBY and TULLIS, 2002), phenomenon which is likely restricted to faults embedded in silica–rich host rocks (e.g., granite). The water in pores, liberated through fracturing during sliding, can be absorbed by the fine particles of silica and wear debris produced by grain fragmentation and refinement, and this will cause the formation of moisture of silica gel (see for instance ILER, 1979). Net effects of the gouge gelation are pore–fluid pressure variation (due to water absorption) and mechanical lubrication of fault surface (due to the gel itself; see next section for more details). At the actual state of the art we do not have sufficient information to write equations describing the gouge evolution. Therefore additional investigations are needed, both in the laboratory and in the field, enabling inclusion of thermal erosion, grain evolution and gouge gelation within a constitutive model.

6. *Mechanical Lubrication and Gouge Acoustic Fluidization*

6.1. *Mechanical Lubrication*

An important effect of the presence of pore fluids within the fault structure is represented by the mechanical lubrication (SOMMERFELD, 1950; SPRAY, 1993; BRODSKY and KANAMORI, 2001; MA *et al.*, 2003). In the model of BRODSKY and KANAMORI (2001) an incompressible fluid obeying the Navier–Stokes equation's flows around the asperity contacts of the fault, without leakage, in the direction perpendicular to the fault surface[7]. In the absence of elastic deformations of the rough surfaces, the fluid pressure in the lubrication model is:

$$p_{fluid}^{(\mathrm{lub})}(\xi_1) = p_{res} + \frac{3}{2}\eta_{fluid} V \int_0^{\xi_1} \frac{w^* - w(\xi_1')}{(w(\xi_1'))^3} d\xi_1', \tag{30}$$

where p_{res} is the initial reservoir pressure (which can be identified with quantity p_{fluid}^{wf} of equation (13)), V is the relative velocity between the fault walls ($2v$ in our notation), $w^* \equiv w(\xi_1^*)$, where ξ_1^* is such that $\left.\frac{\mathrm{d}p_{fluid}^{(lub)}}{\mathrm{d}\xi_1}\right|_{\xi_1=\xi_1^*} = 0$, and ξ_1 maps the length of the lubricated

[7] This is a consequence (HAMROCK, 1994) of the fact that the lubricated zone is much wider than long.

zone $L^{(lub)}$[8]. Qualitatively, $L^{(lub)}$ is equal to the total cumulative fault slip u_{tot}. Interestingly, simple algebra illustrates that if the slipping zone thickness is constant along the strike direction, the lubrication pore fluid pressure is always equal to p_{res}.

The net result of the lubrication process is that the pore fluid pressure is reduced by an amount equal to the last member of equation (30). This in turn can be estimated as

$$P^{(\mathrm{lub})} \cong 12\eta_{fluid}\upsilon \frac{ru_{tot}^2}{(\langle 2w \rangle)^3} \tag{31}$$

where r is the aspect ratio constant for roughness ($r = 10^{-4}$–10^{-2}; Power and Tullis, 1991) and $\langle 2w \rangle$ is the average slipping zone thickness. Therefore equation (2) is rewritten as:

$$\sigma_n^{eff} = \sigma_n - p_{fluid}^{wf} - P^{(lub)}. \tag{32}$$

The fluid pressure can also adjust the fault surface geometry, since

$$2w(\xi_1) = 2w_0(\xi_1) + u^{(\mathrm{lub})}(\xi_1), \tag{33}$$

where $2w_0$ is the initial slipping zone profile and $u^{(lub)}$ is elasto–static displacement caused by lubrication (see equation (8) in Brodsky and Kanamori, 2001). Equation (33) can be approximated as

$$\langle 2w \rangle = \langle 2w_0 \rangle + \frac{P^{(\mathrm{lub})}L}{E} \tag{34}$$

E being the Young' s modulus. $u^{(lub)}$ is significant if $L^{(lub)}$ (or u_{tot}) is greater than a critical length, defined as (see also Ma *et al.*, 2003):

$$L_c^{(\mathrm{lub})} = 2\langle 2w_0 \rangle \left(\frac{\langle 2w_0 \rangle E}{12\eta_{fluid}\upsilon r} \right)^{\frac{1}{3}}. \tag{35}$$

otherwise the slipping zone thickness does not widen. If $u_{tot} > L_c^{(lub)}$ then $P^{(lub)}$ is the positive real root of the following equation

$$P^{(\mathrm{lub})} \left(\langle 2w_0 \rangle + \frac{P^{(\mathrm{lub})}u_{tot}}{E} \right)^3 - 12\eta_{fluid}\upsilon r u_{tot}^2 = 0. \tag{36}$$

It is clear from equation (32) that lubrication contributes to reduce the fault traction (and therefore to increase the fault slip velocity, which in turn further increases $P^{(lub)}$, as stated in equation (31)). Moreover, if lubrication increases the slipping zone thickness, then it will reduce asperity collisions and the contact area between the asperities (which in turn will tend to decrease $P^{(lub)}$, as still stated in equation (31)).

It is generally assumed that when effective normal stress vanishes then material interpenetration and/or tensile (i.e., mode I) cracks (Yamashita, 2000;

[8] The length of the lubricated zone $L^{(lub)}$ is defined as the length over which $p_{fluid}^{(lub)}$ returns to p_{res} level.

DALGUER *et al.*, 2003) develop, leading to the superposition during an earthquake event of all three basic modes of fracture mechanics (ATKINSON, 1987; ANDERS and WILTSCHKO, 1994; PETIT and BARQUINS, 1988). An alternative mechanism that can occur when σ_n^{eff} falls to zero, if fluids are present in the fault zone, is that the frictional stress of contacting asperities described by the Amonton' s Law (1) becomes negligible w. r. to the viscous resistance of the fluid and the friction can be therefore expressed as

$$\tau = \frac{\langle 2w \rangle}{u_{tot}} P^{(\mathrm{lub})} \tag{37}$$

which describes the fault friction in the hydrodynamic regime. Depending on the values of u_{tot} and v, in equation (37) $P^{(lub)}$ is alternatively expressed by (31) or by the solution of (36). For typical conditions ($\langle\, 2w_0 \,\rangle = 1$ mm, $E = 5 \times 10^4$ Pa, $v = 1$ m/s, $u_{tot} = 2$ m, $r = 10 \times 10^{-3}$ m), if the lubricant fluid is water ($\eta_{fluid} = 1 \times 10^{-3}$ Pa s), then $u_{tot} < L_c^{(lub)}$ and (from equation (31)) $P^{(lub)} \cong 4.8 \times 10^4$ Pa. Therefore the lubrication process is negligible in this case and the net effects of the fluid presence within the fault structure will result in thermal pressurization only. On the contrary, if the lubricant fluid is a slurry–formed form the mixture of water and refined gouge ($\eta_{fluid} = 10$ Pa s), then $u_{tot} > L_c^{(lub)}$ and (from equation (36)) $P^{(lub)} \cong 34.9$ MPa, which can be a significant fraction of tectonic loading σ_n. In this case hydro–dynamical lubrication can coexist with thermal pressurization: In a first stage of the rupture, characterized by the presence of ample aqueous fluids, fluids can be squeezed out of the slipping zone due to thermal effects. In a next stage of the rupture, the gouge, rich of particles, can form the slurry with the remaining water; at this moment thermal pressurization is not possible but lubrication effects will become paramount. This is an example of how two different physical mechanisms can be incorporated in a single frictional model.

6.2. *Gouge Acoustic Fluidization*

Another phenomenon which involves the gouge is its acoustic fluidization (MELOSH, 1979, 1996): acoustic waves (high–frequency vibrations) in incoherent rock debris can momentarily decrease the overburden pressure (i.e., normal stress) in some regions of the rocks, allowing sliding in the unloaded regions. It is known that vibrations can allow granular material to flow like liquids and acoustically fluidized debris behaves like a Newtonian fluid. From energy balance considerations, MELOSH (1979) established that acoustic fluidization will occur within a fluidized thickness

$$w_{af} \leq \frac{\tau e u_{tot} v_S^2}{K_M \rho_{rock} g^2 H^2}, \tag{38}$$

where e is the seismic efficiency (typically $e \approx 0.5$), v_S is the S–waves velocity, K_M is a constant ($K_M = 0.9$), ρ_{rock} the cubic mass density of rocks, g is the acceleration of gravity and H is the overburden thickness. For typical conditions, MELOSH (1996) found $w_{af} \leq 20$ m, which can be easily satisfied in mature faults (see also section 2). We notice that this phenomenon does not require the initial presence of fluid within the fault structure and can be regarded as an alternative w. r. to the above–mentioned processes of thermal pressurization in the attempt to explain the weakness of the faults. Unfortunately, it is difficult to detect evidence of fluidization of gouge in exhumed fault zones because signatures of this process generally are not preserved.

7. *Normal Stress Changes and Inelastic Deformations*

7.1. *Bi–material Interface*

Traditional and pioneering earthquake models (see for instance BRACE and BYERLEE, 1966; SAVAGE and WOOD, 1971) simply account for the reduction of the frictional coefficient from its static value to the kinetic frictional level, taking the effective normal stress constant over the duration of the process. Subsequently, WEERTMAN (1980) suggested that a reduction in σ_n during slip between dissimilar materials can influence the dynamic fault weakening. Considering an asperity failure occurring on a bi–material, planar interface separating two uniform, isotropic, elastic half spaces, HARRIS and DAY (1997; their equation (A12)) analytically demonstrated that σ_n can change in time. On the other hand, a material property contrast is not a rare phenomenon in natural faults: LI *et al*. (1990), HOUGH *et al*. (1994) and LI and VIDALE (1996) identified certain strike–slip faults in which one side is embedded in a narrow, fault parallel, low–velocity zone (the width of a few hundred meters). Simultaneously several authors (LEES, 1990; Michael and EBERHART–PHILLIPS, 1991; MAGISTRALE and SANDERS, 1995) inferred the occurrence of significant velocity contrasts across faults, generally less than 30% (e.g., TANIMOTO and SHELDRAKE, 2002).

Even if RENARDY (1992) and ADAMS (1995) theoretically demonstrated that Coulomb frictional sliding is unstable if it occurs between materials with different properties, there is not a general consensus regarding the importance of the presence of bi–material interface on natural earthquakes (BEN–ZION, 2006 vs. ANDREWS and HARRIS, 2005 and HARRIS and DAY, 2005). More recently, DUNHAM and RICE (2008) showed that spatially inhomogeneous slip between dissimilar materials alters σ_n^{eff} (with the relevant scale over which poroelastic properties are to be measured being of the order of the hydraulic diffusion length, which is mm to cm for large earthquakes). Moreover, it is known that the contrast in poroelastic properties (e.g., permeability) across faults can alter both σ_n and p_{fluid} (while the elastic mismatch influences only σ_n).

7.2. *Inelastic Deformations*

Calculations by POLIAKOV *et al*. (2002) and RICE *et al*. (2005) suggested that when the rupture tip passes by, the damage zone is inelatically deformed, even if the primary shear is confined to a thin zone (see Fig. 1). These inelastic deformations, that are a consequence of the high stress concentration near the tip, are likely interacting with the stress evolution and energy flow of the slipping process; therefore they are able to modify the magnitude of traction on the fault. In particular, TEMPLETON and RICE (2008) numerically showed that the accumulation of off–fault plastic straining can delay or even prevent the transition to super–shear rupture velocities. In his numerical simulations of a spontaneously growing 2–D, mode II crack having uniform stress drop, ANDREWS (2005) demonstrated that the energy absorbed off the fault is proportional to the thickness of the plastic strain zone, and therefore to rupture propagation distance[9]. He also showed that the energy loss in the damage zone contributes to the so–called fracture energy, which in turn determines the propagation velocity of a rupture. YAMASHITA (2000), employing a finite–difference method, and DALGUER *et al*. (2003), using a discrete element method, modelled the generation of off–fault damage as the formation of tensile cracks, which is in agreement with the high velocity friction experiments by HIROSE and BYSTRICKY (2007).

8. Discussion

8.1. The Prominent Effects of Temperature on Fault Weakening

In the previous sections we have emphasized that one of the most important effects on fault friction evolution is that of temperature, which might cause pressurization of pore fluids present in the fault structure (see section 3.2), flash heating (section 3.3), melting (see section 3.4), material property changes (see section 3.5.1) and chemical reactions (see section 3.5.2). Assuming that the microscopic processes controlling the direct effect of friction and its decay are thermally activated and follow an Arrhenius relationship, CHESTER (1994, 1995; see also BLANPIED *et al*., 1995) directly incorporated the temperature dependence in the analytical expression of the governing law, proposing a rate–, state– and temperature–dependent version of the Dieterich' s Law (DIETERICH, 1979):

$$
\begin{aligned}
\tau &= \left[\mu_* - a\ln\left(\frac{\upsilon_*}{\upsilon}\right) + \frac{E_a^{(a)}}{R}\left(\frac{1}{T}-\frac{1}{T_*}\right) + b\Psi\right]\sigma_n^{eff} \\
\frac{\mathrm{d}}{\mathrm{d}t}\Psi &= -\frac{\upsilon}{L}\left[\Psi - \ln\left(\frac{\upsilon_*}{\upsilon}\right) + \frac{E_a^{(b)}}{R}\left(\frac{1}{T}-\frac{1}{T_*}\right)\right]
\end{aligned}
\tag{39}
$$

where $E_a^{(a)}$ and $E_a^{(b)}$ are the activation energies for the direct and evolution effect, respectively ($E_a^{(a)} = 60$–154 kJ/mol; $E_a^{(b)} = 43$–168 kJ/mol), and T_* is a reference (i.e., initial) temperature. As in the model of Linker and DIETERICH (1992), a variation in the

[9] In his model, the stress components are first incremented elastically through time. If Coulomb yield criterion is violated, then they are reduced by a time–dependent factor, accounting for Maxwellian visco–plasticity, so that the maximum shear stress resolved over all orientations is equal to the yield stress.

third independent variable (T in this case) will cause explicit and implicit (through the evolution equation for Ψ) changes to the fault friction. We also recall here that a direct effect is also controlled by temperature through the relation (Nakatani, 2001)

$$a = \frac{k_B T_{ac}}{V_a h}, \tag{40}$$

where k_B is the Boltzmann constant ($k_B = 1.38 \times 10^{-23}$ J/K), T_{ac} is the absolute temperature of contacts, V_a is the activation volume ($V_a \sim 10^{-29}$ m^3) and h is the hardness ($h = A_m \sigma_n / A_{ac}$; $h \sim$ GPa), which in turn may decrease with T_{ac} due to plastic deformation of contacts. Additionally, nonuniform temperature distributions in contacting bodies can lead to thermo–elastic deformations, which in turn might modify the contact pressure and generate normal vibrations and dynamic instabilities, the so–called frictionally–excited thermo–elastic instability (TEI; e.g., Barber, 1969).

8.2. *Scaling Problems and Related Issues*

It has been mentioned that each nonlinear dissipation process that can potentially act during an earthquake rupture has its own distance and time scales, which can be very different from one phenomenon to another. The difference in scale lengths, as well as the problem of the scale separation, can represent a limitation in the attempt to simultaneously incorporate *all* the mechanisms described in this paper in a single constitutive model. In the paper we have seen that thermal pressurization (section 3.2) can coexist with mechanical lubrication (section 6.1) as well as with porosity (section 4.1) and permeability evolutions (section 4.2). The same holds for flash heating and thermal pressurization (Noda *et al*., 2009). This simultaneous incorporation ultimately leads to numerical problems, often severe, caused by the need to properly resolve the characteristic distances and times of each separate process. The concurrent increase in computational power and the development of new numerical algorithms can definitively assist us in this effort.

Table 2 reports a synoptic view of the characteristic length scales for the processes described in this paper. Two important lengths (see for instance Bizzarri *et al*., 2001), that are not negligible w. r. to the other scale lengths involved in the breakdown process, are the breakdown zone length (or size, X_b) and the breakdown zone time (or duration, T_b). They quantify the spatial extension, and time duration, of the cohesive zone, respectively; in other words they express the amount of cumulative fault slip, and the elapsed time, required to the friction to drop, in some way, from the yield stress down to the residual level.

Another open problem is related to the difficulty in moving from the scale of the laboratory (where samples are of the order of several meters) up to the scale of real faults (typically several kilometers long). Many phenomena described in the paper have been measured in the lab: This raises the problem of how to scale the values of the parameters of the inferred equations to natural faults. Both geological observations and improve-

Table 2

Synoptic view of the characteristic distances and scale lengths of the processes described in the paper

Process	Characteristic distance Scale length	Typical value range
Macroscopic decrease of fault traction from yield stress to residual level	d_0 X_b	$\sim$ few mm in the lab[(a), (b)] $\sim$ 100 of m[(c)]
Temporal evolution of the state variable in the framework of the rate– and state–dependent friction laws	L	$\sim$ few μm in the lab[(b)]
Thermal pressurization (section 3.2)	$2w$ $\delta = \sqrt{2\chi t_d}$	$\leq$ 1 cm[(d)] $\sim$ few cm
Flash heating (section 3.3)	D_{ac}	$\sim$ few μm
Gouge and rocks melting (section 3.4)	$2w_{melt}$	$\sim$ 100 of μm in the lab
Porosity evolution (section 4.1):		
– equations (18) to (20)	$2w$	$\leq$ 1 cm[(d)]
– equations (21) and (22)	L_{SR}	assumed to be equal to L
Gouge acoustic fluidization (section 6.2)	w_{af}[(e)]	20 m

[(a)] See also OHNAKA (2003)
[(b)] These estimates refer to an idealized fault of zero thickness (i.e., bare surfaces)
[(c)] Estimates from numerical 3–D fault models of BIZZARRI and COCCO (2005). In each fault node, the breakdown zone time, T_b, is associated to X_b through the local rupture velocity v_r via: $T_b = X_b/v_r$
[(d)] From geological estimates SUPPE (1985) and CHESTER and CHESTER (1998)
[(e)] Acoustic fluidization is effective for thicknesses lower than w_{af} (theoretical estimates by Melosh, 1996)

ments in laboratory machines are necessary ingredients in our understanding of earthquake source physics and our capability to reproduce it numerically.

9. *Conclusions*

Earthquake models can help us in the attempt to understand how a rupture starts to develop and propagate, how seismic waves travel in the Earth crust and how high frequency radiation can affect a site on the ground. Since analytical, closed–form analytical solutions of the fully dynamic, spontaneous rupture problem do not exist (even in homogeneous conditions), it is clear that accurate and realistic numerical simulations are the only available path. In addition to the development of robust and capable computer codes, the solution of the elasto-dynamic problem requires the introduction of a fault governing law, which ensures that the energy flux is bounded at the crack tip and prevents the presence of singularities of solutions at the rupture front. At the present state of the art, unfortunately, among the different possibilities presented in the literature, the most appropriate form of the physical law that governs fault during its seismic cycle is not agreed upon. This is particularly true for the traction evolution within the coseismic temporal scale, where the stress release and the consequent emission of seismic waves are realized.

In this paper we have presented and discussed a large number of physical mechanisms that can potentially take place during an earthquake event. These phenomena are macroscopic, in that fundamental variables (i.e., the physical observables) describing them have to be regarded as macroscopic averages (see also OHNAKA, 2003). As a result, the fault friction does not formally describe the stress acting on each single asperity, but the macroscopic average of the stress acting within the slipping zone. The same holds for the sliding velocity: v is the macroscopic slip rate and not the microscopic one, at solid–solid contacts. Unlikely, a link between the microphysics of materials, described in terms of lattice or atomic properties, and the macrophysical description of friction, obtained from stick–slip laboratory experiments, is missing. On the other hand, we cannot expect to be able to mathematically (either deterministically or statistically) describe the evolution of all the surface asperities and of all micro cracks in the damage zone.

Recent laboratory experiments and geological investigations have clearly shown that different dissipative processes can lead to the same steady state value of friction. In the simple approximation which considers only one single event on an isolated fault, some authors claim that the slip dependence is paramount (e.g., OHNAKA, 2003). On the other hand, the explicit dependence of friction on sliding velocity (e.g., DIETERICH, 1986) is unquestionable, even at high slip rates (e.g., TSUTSUMI and SHIMAMOTO, 1997). In fact, in the literature there is a major debate (see for instance BIZZARRI and COCCO, 2006d) concerning the most important dependence of fault friction. Actually, the problem of what is (are) the dominant physical mechanism(s) controlling the friction evolution (i.e., the quantitative estimate of the weights w_i in equation (3)) is still unsolved.

We believe that seismic data presently available are not sufficient to clarify what specific mechanism is operating (or dominant) during a specific earthquake event. The inferred traction evolution on the fault, as retrieved from seismological records (e.g., IDE and TAKEO, 1997; GUATTERI and SPUDICH, 2000), gives us only some general information about the average weakening process on an idealized mathematical fault plane. Moreover, it is affected by the unequivocal choice of the source time function adopted in kinematic inversions and by the frequency band limitation in data recording (SPUDICH and GUATTERI, 2004) and sometimes could be inconsistent with dynamic ruptures (PAGE *et al.*, 2005). On the other side, we have seen in previous sections that the insertion of additional physical and chemical mechanisms in the analytical expression of a fault governing equation cannot be neglected *a priori*. The first reason is that, compared to results obtained by adopting a simplified or idealized constitutive relation (where effective normal stress is assumed to be constant and where, for instance, only slip or slip rate dependence is postulated), numerical experiments from models in which additional physical mechanisms are accounted for show a significant, often dramatic, change in the dynamic stress drop (and therefore in the resulting ground motions), in the distance over which it is realized, in the so–called fracture energy and in the total scalar seismic moment. The second reason is that, as we have shown in the paper, the inclusion of different mechanisms in some cases requires a modification of its usual, or classical, analytical expression (recall the effects of gouge and rocks melting and those of hydrodynamic lubrication).

As a future perspective, it would be intriguing—and at the same time extraordinarily challenging—to try to compare synthetics, both on the fault and out of the fault, obtained by assuming that one particular physical mechanism is paramount w. r. to the others, in order to look for some characteristic signatures and specific features in the solutions and eventually attempt to envisage such features in real seismological data.

Moreover, we are inclined to think that only a multidisciplinary approach to source mechanics, which combines results from accurate theoretical models, advanced laboratory experiments, systematic field observations and data analyses, can eventually lead to the formulation of a realistic fault governing model and can assist us in the ambitious aim of describing as realistically as possible the complexity of the breakdown process during an earthquake rupture. In this paper we have underlined that some different, nonlinear, chemico–physical processes can potentially cooperate, interact, or even compete one with each other. We have shown that in most cases we are able to write equations describing them (sometimes with constrained parameters), and we have explicitly indicated how they can be incorporated into a fault governing model. In order to reproduce the complexity and the richness of the inelastic and dissipative mechanisms occurring on a fault surface during an earthquake event, a "classical" constitutive relation appears to be currently inadequate and the above–mentioned multidisciplinary approach would be painstakingly considered for years to come.

Acknowledgements

The Euro–Conference on Rock Physics and Geomechanics "Natural hazards: thermo–hydro–mechanical processes in rocks" held in Erice in September 2007 motivated this work and the Director of the School, Enzo Boschi, and the Directors of the course, Sergio Vinciguerra and Yves Bernabé, are kindly acknowledged. Moreover, I benefitted from insightful discussions with Renata Dmowska, Eric Dunham, Yann Klinger, Laurent Montési, Jim Rice, Paul Segall and Paul Spudich. Comments by Emily Brodsky concerning mechanical lubrication are also greatly appreciated. I lastly acknowledge Chris Marone and Massimo Cocco for their reviews.

References

Abercrombie, R. E. and Rice, J. R. (2005), *Can observations of earthquake scaling constrain slip weakening?*, Geophys. J. Int. *162*, 406–424.

Adams, G. G. (1995), *Self-excited oscillations of two elastic half–spaces sliding with a constant coefficient of friction*, J. Appl. Mech. *62*, 867–871.

Aki, K. (1972), *Earthquake mechanism*, Tectonophys. *13*, 423–446.

Aki, K. (1979), *Characterization of barriers on an earthquake fault*, J. Geophys. Res. *84*, B11, 6140–6148.

Anders, M. H. and Wiltschko, D. V. (1994), *Microfracturing, paleostress and the growth of faults*, J. Struct. Geol. *16*, 795–815.

Andrews, D. J. (1994), *Dynamic growth of mixed–mode shear cracks*, Bull. Seism. Soc. Am. *84*, 4, 1184–1198.

ANDREWS, D. J. (2002), *A fault constitutive relation accounting for thermal pressurization of pore fluid*, J. Geophys. Res. *107*, B12, 2363, doi: 10.1029/2002JB001942.

ANDREWS, D. J. (2005), *Rupture dynamics with energy loss outside the slip zone*, J. Geophys. Res. *110*, B01307, doi: 10.1029/2004JB003191.

ANDREWS, D. J. and HARRIS, R. A. (2005), *The wrinkle–like slip pulse is not important in earthquake dynamics*, *Geophys.* Res. Lett. *32*, L23303, doi:10.1029/2005GL023996.

ANTONIOLI, A., BELARDINELLI, M. E., BIZZARRI, A., and VOGFJORD, K. S. (2006), *Evidence of instantaneous dynamic triggering during the seismic sequence of year 2000 in south Iceland*, J. Geophys. Res. *111*, B03302, doi: 10.1029/2005JB003935.

ATKINSON, B. K. *Fracture Mechanics of Rock*, (Academic, San Diego, CA. 1987).

BAK, P., TANG, C., and WIESENFLED, K. (1987), *Self–organized criticality: An explanation of the 1/f noise*, Phys. Rev. Lett. *59*, 381–384.

BARBER, J. R. (1969), *Thermoelastic instabilities in the sliding of conforming solids*, Proc. Roy. Soc. (London) *A312*, 381–394.

BEELER, N. M., TULLIS, T. E. and WEEKS, J. D. (1994), *The roles of time and displacement in the evolution effect in rock friction*, Geophys. Res. Lett. *21*, 18, 1987-1990.

BEN–ZION, Y. (2006), *A comment on "Material contrast does not predict earthquake rupture propagation direction" by R. A. Harris and S. M Day*. Geophys. Res. Lett. *33*, L13310, doi:10.1029/2005GL025652.

BEN–ZION, Y. and Sammis, C. G. (2003), *Characterization of fault zones*, Pure Appl. Geophys. *160*, 677–715.

BENIOFF, H. (1951), *Earthquakes and rock creep Part I: Creep characteristics of rocks and the origin of aftershocks*, Bull. Seism. Soc. Amer. *41*, 31–62.

BHAT, H. S., DMOWSKA, R., KING, G. C. P., KLINGER, Y., and RICE, J. R. (2007), *Off–fault damage patterns due to supershear ruptures with application to the 2001 M_w 8.1 Kokoxili (Kunlun) Tibet earthquake*, J Geophys Res. *112*, B06301, doi: 10.1029/2006JB004425.

BILLI, A. and STORTI, F. (2004), *Fractal distribution of particle size in carbonate cataclastic rocks from the core of a regional strike–slip fault zone*, Tectonophys. *384*, 115–128.

BIZZARRI, A. and BELARDINELLI, M. E. (2008), *Modelling instantaneous dynamic triggering in a 3–D fault system: Application to the 2000 June South Iceland seismic sequence*, Geophys. J. Intl. *173*, 906–921, doi: 10.1111/j.1365-246X.2008.03765.x.

BIZZARRI, A. and COCCO, M. (2004), *Thermal pressurization in 3–D dynamic spontaneous rupture models with cohesive zone*, EOS Trans. AGU, *85*, No. 47, Fall Meet. Suppl., Abstract T23A–0572.

BIZZARRI, A. and COCCO, M. (2005), *3D dynamic simulations of spontaneous rupture propagation governed by different constitutive laws with rake rotation allowed*, Annals of Geophys. *48*, 2, 277–299.

BIZZARRI, A. and COCCO, M. (2006a), *A thermal pressurization model for the spontaneous dynamic rupture propagation on a three–dimensional fault: 1. Methodological approach*, J. Geophys. Res. *111*, B05303, doi: 10.1029/2005JB003862.

BIZZARRI, A. and COCCO, M. (2006b), *A thermal pressurization model for the spontaneous dynamic rupture propagation on a three–dimensional fault: 2. Traction evolution and dynamic parameters*, J. Geophys. Res. *111*, B05304, doi: 10.1029/2005JB003864.

BIZZARRI, A. and COCCO, M. (2006c), *Correction to "A thermal pressurization model for the spontaneous dynamic rupture propagation on a three–dimensional fault: 1. Methodological approach"*, J. Geophys. Res. *111*, B11302, doi: 10.1029/2006JB004759.

BIZZARRI, A. and COCCO, M. (2006d), *Comment on "Earthquake cycles and physical modeling of the process leading up to a large earthquake"*, Earth Planets Space *58*, No. 11, 1525–1528.

BIZZARRI, A., COCCO, M., ANDREWS, D. J., and BOSCHI, E. (2001), *Solving the dynamic rupture problem with different numerical approaches and constitutive laws*, Geophys. J. Int. *144*, 656-678.

BIZZARRI, A. and SPUDICH, P. (2008), *Effects of supershear rupture speed on the high-frequency content of S waves investigated using spontaneous dynamic rupture models and isochrone theory*, J. Geophys. Res. *113*, B05304, doi: 10.1029/2007JB005146.

BLANPIED, M. L., LOCKNER, D. A., and BYERLEE, J. D. (1995), *Frictional slip of granite at hydrothermal conditions*, J. Geophys. Res. *100*, B7, 13,045–13,064.

BOLEY, B. A. and WEINER, J. H. *Theory of Thermal Stresses* (Krieger, Malabar 1985).

Brace, W. F. (1978), *A note on permeability changes in geologic material due to stress*, Pure Appl. Geophys. *116*, 627–633.

Brace, W. F. and Byerlee, J. D. (1966), *Stick–slip as a mechanism for earthquakes*, Science *153*, 3739, 990–992.

Brace, W. F., Walsh, J. B., and Frangos, W. T. (1968), *Permeability of granite under high pressure*, J. Geophys. Res. *73*, 6, 2225–2236.

Brodsky, E. E. and Kanamori, H. (2001), *Elastohydrodynamic lubrication of faults*, J. Geophys. Res. *106*, B8, 16,357–16,374.

Byerlee, J. D. (1978), *Friction of rocks*, Pure Appl. Geophys. *116*, 615–626.

Cardwell, R. K., Chinn, D. S., Moore, G. F., and Turcotte, D. L. (1978), *Frictional heating on a fault zone with finite thickness*, Geophys J. Roy. Astr. Soc. *52*, 525–530.

Carman, P. C. (1937), *Fluid flow through granular beds*, Trans. Inst. Chem. Eng. 15,150.

Carman, P.C. *Flow of Gases through Porous Media* (Butterworths Scientific Publications, London 1956).

Cashman, S. M., Baldwin, J. N., Cashman, K. V., Swanson, K., and Crawford, K. (2007), *Microstructures developed by coseismic and aseismic faulting in near-surface sediments, San Andreas fault, California*, Geology *35*, 611–614, doi: 10.1130/G23545A.

Chester, F. M. (1994), *Effects of temperature on friction: Constitutive equations and experiments with quartz gouge*, J. Geophys. Res. *99*, 7247–7262.

Chester, F. M. (1995), *A rheologic model for wet crust applied to strike–slip faults*, J. Geophys. Res. *100*, B7, 13,033–13,044.

Chester, F. M. and Chester, J. S. (1998) *Ultracataclasite structure and friction processes of the Punchbowl fault, San Andreas system, California*, Tectonophys. *295*, 199–221.

Chester, F. M., Chester, J. S., Kirschner, D. L., Schulz, S. E., and Evans, J. P. *Structure of large-displacement, strike-slip fault zones in the brittle continental crust*. In *Rheology and Deformation in the Lithosphere at Continental Margins* (eds. G. D. Karner, B. Taylor, N. W. Driscoll, and D. L. Kohlstedt) pp. 223–260 (Columbia Univ. Press, New York 2004).

Clauser, C. and Huenges, E. (2000), *Thermal conductivity of rocks and minerals*, In *Rock Physics and Phase Relations*, AGU Ref. Shelf, vol. 3 (ed. T. J. Ahrens), pp. 105–126 (AGU, Washington, D. C. 2000).

Cocco, M. and Bizzarri, A. (2002), *On the slip–weakening behavior of rate– and state–dependent constitutive laws*, Geophys. Res. Lett. *29*, 11, doi: 10.1029/2001GL01399.

Dalguer, L. A., Irikura, K., and Riera, J. D. (2003), *Simulation of tensile crack generation by three–dimensional dynamic shear rupture propagation during an earthquake*, J. Geophys. Res. *108*, B3, 2144, doi:10.1029/2001JB001738.

Day, S. M. (1982), *Three-dimensional finite difference simulation of spontaneous rupture: the effect of nonuniform prestress*, Bull. Seism. Soc. Am. *72*, 1881–1902.

Das, S. and Aki, K. (1977a), *A numerical study of two–dimensional spontaneous rupture propagation, Geophys*, J. Roy. Astr. Soc. *50*, 643–668.

Das, S. and Aki, K. (1977b), *Fault plane with barriers: a versatile earthquake model*, J. Geophys. Res. *82*, 36, 5658–5670.

Dieterich, J. H. (1979), *Modeling of rock friction: 1. Experimental results and constitutive equations*, J. Geophys. Res. *84*, 2161–2168.

Dieterich, J. H. (1986), *A model for the nucleation of earthquake slip*, In *Earthquake Source Mechanics, Geophysical Monograph*, *37*, *Maurice Ewing Series*, 6 (ed. S. Das, J. Boatwright and H. Scholz), (Am. Geophys. Union, Washington D. C. 1986) pp. 37–47.

Dunham, E. M. and Rice, J. R. (2008), *Earthquake slip between dissimilar poroelastic materials*, J. Geophys. Res. *113*, B09304, doi: 10.1029/2007JB005405.

Engelder, J. T. (1974), *Cataclasis and the generation of fault gouge*, Geol. Soc. Amer. Bull. *85*, 1515–1522.

Evans, J. P. and Chester, F. M. (1995), *Fluid–rock interaction in faults of the San Andreas system: Inferences from San Gabriel fault rock geochemistry and microstructures*, J. Geophys. Res. *100*, 13,007–13,020.

Fialko, Y. A. (2004), *Temperature fields generated by the elastodynamic propagation of shear cracks in the Earth*, J. Geophys. Res. *109*, No. B01303, doi: 10.1029/2003JB002497.

Fialko, Y. and Khazan, Y. (2005), *Fusion by the earthquake fault friction: stick or slip?* J. Geophys. Res. *110*, B12407 doi.org/10.1029/2005JB003869.

Fliss, S., Bhat, H. S., Dmowska, R., and Rice, J. R. (2005), *Fault branching and rupture directivity*, J. Geophys. Res. *110*, B06312, doi: 10.1029/2004JB003368.

Goldsby, D. L. and Tullis, T. E. (2002), *Low frictional strength of quartz rocks at subseismic slip rates*, Geophys. Res. Lett. *29*, 17, doi: 10.1029/2002GL015240.

Guatteri, M. and Spudich, P. (2000), *What can strong-motion data tell us about slip-weakening fault-friction laws?* Bull. Seism. Soc. Am. *90*, 1, 98-116.

Hamrock, B. J. (1994), *Fundamentals of Fluid Film Lubrication* (McGraw Hill, New York 1994).

Han, R., Shimamoto, T., Hirose, T., Ree, J.–H., and Ando, J.–I. (2007), *Ultralow friction of carbonate faults caused by thermal decomposition*, Science *316*, 878–881.

Hanks, T. C. (1977), *Earthquake stress drop, ambient tectonic stresses, and stresses that drive plate motion*, Pure Appl. Geophys. *115*, 441–458.

Harris, R. A. and Day, S. M. (1997), *Effects of a low-velocity zone on a dynamic rupture*, Bull. Seismol. Soc. Am. *87*, 1267–1280.

Harris, R. A. and Day, S. M. (2005), *Material contrast does not predict earthquake rupture propagation direction*, Geophys. Res. Lett. *32*, L23301, doi:10.1029/2005GL023941.

Heermance, R., Shipton, Z. K., and Evans, J. P. (2003), *Fault structure control on fault slip and ground motion during the 1999 rupture of the Chelungpu Fault, Taiwan*, Bull. Seismol. Soc. Am. *93*, 3, 1034–1050.

Hirose, T. and Bystricky, M. (2007), *Extreme dynamic weakening of faults during dehydration by coseismic shear heating*, Geophys. Res. Lett. *34*, L14311, doi:10.1029/2007GL030049.

Hirose, T. and Shimamoto, T. (2003), *Fractal dimension of molten surfaces as a possible parameter to infer the slip–weakening distance of faults from natural pseudotachylytes*, J. Struct. Geol. *25*, 1569–1574.

Hough, S. E., Ben–Zion., Y., and Leary, P. (1994), *Fault–zone waves observed at southern Joshua Tree earthquake rupture zone*, Bull. Seism. Soc. Am. *84*, 761–767.

Huenges, E., and Will, G. *Permeability, bulk modulus and complex resistivity in crystalline rocks*, In *Fluids Movements – Element Transport and the Composition of the Deep Crust,* (Ed. D. Bridgwater) pp. 361–375, (Kluwed, Dordrecht 1989).

Ida, Y. (1972), *Cohesive force across the tip of a longitudinal-shear crack and Griffith' s specific surface energy*, J. Geophys. Res. *77*, 20, 3796–3805.

Ide, S. and Takeo, M. (1997), *Determination of constitutive relations of fault slip based on seismic wave analysis*, J. Geophys. Res. *102*, B12, 27,379-27,391.

Iler, R. K. *The Chemistry of Silica* (John Wiley and Sons, New York 1979), 866 pp

Jeffreys, H. (1942), *On the mechanics of faulting*, Geological Magazine *79*, 291–295.

Jourde, H., Flodin, E. A., Aydin, A., Durlofsky, L. J. and Wen, X. H. (2002), *Computing permeability of fault zones in eolian sandstone from outcrop measurements*, AAPG Bull. *86*, 1187–1200.

Kame, N., Rice, J. R., and Dmowska, R. (2003), *Effects of pre–stress state and rupture velocity on dynamic fault branching*, J. Geophys. Res. 108, B5, 2265, doi: 10.1029/2002JB002189.

Kanamori, H. and Stewart, G. S. (1976), *Mode of strain release along Gibbs fracture zone, Mid-Atlantic ridge,* Phys. Earth and Plan. Interiors, *11* (4), 312–332.

Kanamori, H. and Heaton, T. H. (2000), *Microscopic and macroscopic physics of earthquakes*, GeoComplexity and the Physics of Earthquakes–Geophysical Monograph *120*, 147–163.

Klinger, Y., Xu, X., Tapponnier, P., Van der Woerd, J., Laserre, C., and King, G. (2005), *High–resolution satellite imagery mapping of the surface rupture and slip distribution of the $M_w \sim 7.8$, November 14, 2001 Kokoxili earthquake* (Kunlun fault, Northern Tibet, China), Bull. Seis. Soc. Am. *95*, 5, 1970–1987.

Kozeny, J. (1927), *Uber kapillare Leitung des wassers in Böden*, Sitzungsber. Akad. Wiss. Wien Math. Naturwiss. Kl., Abt. 2a, 136,271–306 (In German).

Krajcinovic, D. (1993), *Scaling law for the blue cheese model of damaga*, Phys. Lett. A *173*, 433–437.

Lachenbruch, A. H. (1980), *Frictional heating, fluid pressure, and the resistance to fault motion*, J. Geophys. Res. *85*, B11, 6097–6122.

Lee, T. C. and Delaney, P. T. (1987), *Frictional heating and pore pressure rise due to a fault slip*, Geophys. J. Roy. Astr. Soc. *88*, 3, 569–591.

Lees, J. M. (1990), *Tomographic P–wave velocity images of the Loma Prieta earthquake asperity*, Geophys. Res. Lett. *17*, 1433–1436.

LI, Y.–G., LEARY, P., AKI, K., and MALIN, P. (1990), *Seismic trapped modes in the Oroville and San Andreas fault zones*, Science *249*, 763–766.

LI, Y.–G. and VIDALE, J. E. (1996), *Low–velocity fault–zone guided waves: numerical investigations of trapping efficiency*, Bull. Seism. Soc. Am. *86*, 371–378.

LINKER, M. F. and DIETERICH, J. H. (1992), *Effects of variable normal stress on rock friction: observations and constitutive equations*, J. Geophys. Res. *97*, B4, 4923-4940.

LOCKNER, D., NAKA, H., TANAKA, H., ITO, H., and IKEDA, R. (2000), *Permeability and strength of core samples from the Nojima fault of the 1995 Kobe earthquake*. In *Proc. International Workshop on the Nojima Fault Core and Borehole Data Analysis* (eds. H. Ito, K. Fujimoto, H. Tanaka, and D. Lockner), pp. 147–152, U.S. Geol. Surv. Open File Rep., 00–129.

MA, K.-F., BRODSKY, E. E., MORI, J., JI, C., SONG, T.-R. A., and KANAMORI, H. (2003), *Evidence for fault lubrication during the 1999 Chi–Chi, Taiwan, earthquake (M_w 7.6)*, G. Res. Lett. ***30***, 5, 1244, doi: 10.1029/2002GL015380.

MADARIAGA, R. (1979), *On the relation between seismic moment and stress drop in the presence of stress and strength heterogeneity*, J. Geophys. Res. *84*, B5, 2243–2250.

MAGISTRALE, H. and SANDERS, C. (1995), *P–wave image of the Peninsular Ranges batholith, southern California*, Geophys. Res. Lett. *22*, 2549–2552.

MAI, P. M. and BEROZA, G. C. (2002), *A spatial random field model to characterize complexity in earthquake slip*, J. Geophys. Res. *107*, B11, 2308, doi: 10.1029/2001JB000588.

MAIR, K. and MARONE, C. (1999), *Friction of simulated fault gauge for a wide range of slip velocities and normal stresses*, J. Geophys. Res. *104* (B12), 28, 899–28, 914.

MARONE, C. and KILGORE, B. (1993), *Scaling of the critical slip distance for seismic faulting with shear strain in fault zones*, Nature *362*, 618-621.

MARONE, C., RALEIGH, C. B., and SCHOLZ, C. H. (1990), *Frictional behavior and constitutive modeling of simulated fault gouge*, J. Geophys. Res. *95*, B5, 7007–7025.

MASE, C. W. and SMITH, L. (1985), *Pore–fluid pressures and frictional heating on a fault surface*, Pure Appl. Geophys. *92*, 6249–6272.

MASE, C. W. and SMITH, L. (1987), *Effects of frictional heating on the thermal, hydrologic, and mechanical response of a fault*, J. Geophys. Res. *92*, B7, 6249–6272.

MCKENZIE, D. P. (1984), *The generation and compaction of partially molten rock*, J. Petrol. *25*, 713–765.

MCKENZIE, D. and BRUNE, J. (1972), *Melting on fault planes during large earthquakes*, Geophys. J. R. Astron. Soc. *29*, 65–78.

MELOSH, H. J. (1979), *Acoustic fluidization: A new geologic process?* J. Geophys. Res. *84*, B13, 7513–7520.

MELOSH, H. J. (1996), *Dynamical weakening of faults by acoustic fluidization*, Nature *397*, 601–606.

MICHAEL, A. J. and EBERHART–PHILLIPS, D. (1991), *Relations among fault behavior, subsurface geology, and three–dimensional velocity models*, Science *253*, 651–654.

MILLER, S. A., NUR, A., and OLGAARD, D. L. (1996), *Earthquakes as a coupled shear stress–high pore pressure dynamical system*, Geophys. Res. Lett. *23*, 197–200.

MIZOGUCHI, K., HIROSE, T., SHIMAMOTO, T., and FUKUYAMA, E. (2007), *Reconstruction of seismic faulting by high–velocity friction experiments: An example of the 1995 Kobe earthquake*, Geophys. Res. Lett. *34*, L01308, doi: 10.1029/2006GL027931.

NAKATANI, M. (2001), *Conceptual and physical clarification of rate– and state–dependent friction law: Frictional sliding as a thermally activated rheology*, J. Geophys. Res. *106*, 13,347–13,380, doi: 10.1029/2000JB900453.

NIELSEN, S., DI TORO, G., HIROSE, T., and SHIMAMOTO, T. (2008), *Frictional melt and seismic slip*, J. Geophys. Res. *113*, B01308, doi: 10.1029/2007JB005122.

NODA, H., DUNHAM, E. M., and RICE, J. R. (2009), *Earthquake ruptures with thermal weakening and the operation of major faults at low overall stress levels*, submitted to J. Geophys. Res.

NUR, A. and BOOKER, J. (1972), *Aftershocks caused by pore fluid flow?* Science *175*, 885–887.

OHNAKA, M. (2003), *A constitutive scaling law and a unified comprehension for frictional slip failure, shear fracture of intact rocks, and earthquake rupture*, J. Geophys. Res. *108*, B2, 2080, doi: 10.1029/2000JB000123.

Ohnaka, M. (1996), *Nonuniformity of the constitutive law parameters for shear rupture and quasistatic nucleation to dynamic rupture: a physical model of earthquake generation processes*, Proc. Natl. Acad. Sci. USA, *93*, 3795–3802.

Okubo, P. G. (1989), *Dynamic rupture modeling with laboratory-derived constitutive relations*, J. Geophys. Res. *94*, B9, 12,321-12,335.

Page, M. T., Dunham, E. M., and Carlson, J. M. (2005), *Distinguishing barriers and asperities in near–source ground motion,* J. Geophys. Res. *110*, B11302, doi:10.1029/2005JB003736.

Parton, V. Z. and Morozov, E. M. *Elastic-Plastic Fracture Mechanics* (Mir Publishers Moscow, 1974), 427 pp.

Petit, J. P. and Barquins, M. (1988), *Can natural faults propagate under mode II conditions?* Tectonics *7*, 1243–1256.

Pittarello, L., Di Toro, G., Bizzarri, A., Pennacchioni, G., Hadizadeh, J., and Cocco, M. (2008), *Energy partitioning during seismic slip in pseudotachylyte–bearing faults (Gole Larghe Fault, Adamello, Italy)*, Earth Planet Sci. Lett. *269*, 131–139, doi: 10.1016/j.epsl.2008.01.052.

Poliakov, A. N. B., Dmowska, R., and Rice, J. R. (2002), *Dynamic shear rupture interactions with fault bends and off–axis secondary faulting*, J. Geophys. Res. *107*, doi:10.1029/2001JB000572.

Power, W. L. and Tullis, T. E. (1991), *Euclidean and fractal models for the description of rock surface roughness*, J. Geophys. Res. *93*, 415–424.

Power, W. L., Tullis, T. E., and Weeks, D. J. (1988), *Roughness and wear during brittle faulting*, J. Geophys. Res. *93*, B12, 15,268–15,278.

Prakash, V. and Yuan, F. (2004), *Results of a pilot study to investigate the feasibility of using new experimental techniques to measure sliding resistance at seismic slip rates*, EOS Trans. AGU *85*, 47, Fall Meet. Suppl., Abstract T21D-02.

Pratt, H. R., Black, A. D., Brace, W. F., and Swolfs, H. (1977), *Elastic and transport properties an in–situ jointed granite*, Int. J. Rock Mech. Min. Sci. *14*, 35–45.

Ranalli, G. *Rheology of the Earth*, 2nd Ed. (Chapman and Hall, London 1995).

Rathbun, A. P. and Marone, C. (2009), *Effect of strain localization on frictional behaviour of sheared granular materials*, submitted to J. Geophys. Res.

Reid, H. F. *The Mechanics of the Earthquake*, Rept. State Earthquake Inv. Comm., The California Earthquake of April 18, 1906 (Washington D. C. 1910).

Rempel, A. and Rice, J. (2006), *Thermal pressurization and on set of melting in fault zones*, J. Geophys. Res. *111*, B09314, doi:10.1029/2006JB004314.

Renardy, Y. (1992), *Ill–posedness at the boundary for elastic solids sliding under Coulomb–friction*, J. Elasticity *27*, 3, 281–287.

Rice, J. R. *Fault stress states, pore pressure distributions, and the weakness of the San Andreas Fault*. In *Fault Mechanics and Transport Properties in Rocks (the Brace Volume)*, (eds. by B. Evans and T.-F. Wong), (*Academic*, San Diego 1992) pp. 475–503.

Rice, J. R. (2006), *Heating and weakening of faults during earthquake slip*, J. Geophys. Res. *111*, B5, B05311, doi: 10.1029/2005JB004006.

Rice, J. R., Sammis, C. G. and Parsons, R. (2005), *Off–fault secondary failure induced by a dynamic slip–pulse*, Bull. Seism. Soc. Am. *95*, 1, 109–134, doi: 10.1785/0120030166, 2005.

Robertson, E. C. (1983), *Relationship of fault displacement to gouge and breccia thickness*, Mining Engin. *35*, 10, 1426–1432.

Ruina, A. L. (1983), *Slip instability and state variable friction laws*, J. Geophys. Res. *88*, B12, 10,359–10,370.

Sammis, C. G. and Ben–Zion, Y. (2007), *The mechanics of grain-size reduction in fault zones*, submitted to J. Geophys. Res.

Savage, J. C. and Wood, M. D. (1971), *The relation between apparent stress and stress drop*, Bull. Seismol. Soc. Am. *61*, 1381–1388.

Scholz, C. H. (1987), *Wear and gouge formation in brittle fracture*, Geology *15*, 493–495.

Scholz, C. H. and Hanks, T. C. *The strength of the San Andreas fault: A discussion*. In *Rheology and Deformation of the Lithosphere at Continental Margins* (eds. G. D. Karner, B. Taylor and D. Kohlstedt) (Columbia University Press, New York 2004).

SHAPIRO, S. A., PATZIG, R., ROTHERT, E., and RINDSHWENTNER, J. (2003), *Triggering of seismicity by pore–pressure perturbations: Permeability–related signature of the phenomenon*, Pure Appl. Geophys. *160*, 1051–1066.

SEGALL, P. and RICE, J. R. (1995), *Dilatancy, compaction, and slip instability of a fluid–infiltrated fault*, J. Geophys. Res. *100*, 101, 22,155–22,171.

SIBSON, R. H. (1973), *Interaction between temperature and pore–fluid pressure during earthquake faulting – A mechanism for partial or total stress relief*, Nature *243*, 66–68.

SIBSON, R. H. (1986), *Brecciation processes in fault zones: Inferences from earthquake rupturing*, Pure Appl. Geophys. *124*, 169–175.

SIBSON, R. H. (2003), *Thickness of the seismic slip zone*, Bull. Seism. Soc. Am. *93*, 3, 1169–1178.

SIBSON, R. and TOY, V. *The habitat of fault-generated pseudotachylyte: Presence vs. absence of friction melt*. In *Radiated Energy and the Physics of Earthquake Faulting* (eds. R. Abercrombie, A. McGarr, H. Kanamori, and G. Di Toro), (AGU, Washington, D. C. 2006).

SLEEP, N. H. (1995), *Ductile creep, compaction, and rate and state dependent friction within major fault zones*, J. Geopys. Res. *100*, B7, 13,065–13,080.

SLEEP, N. H. (1997), *Application of a unified rate and state friction theory to the mechanics of fault zones with strain localization*, J. Geophys. Res. *102*, B2, 2875-2895.

SLEEP, N. H. (1999), *Rate– and state–dependent friction of intact rock and gouge*, J. Geophys. Res. *104*, B8, 17,847-17,855.

SLEEP, N. H. and Blanpied, M. L. (1992), *Creep, compaction and the weak rheology of major faults*, Nature *359*, 687–692.

SOMMERFELD, A. *Mechanics of Deformable Bodies* (Academic Press, San Diego, CA 1950).

SPRAY, J. G. (1993), *Viscosity determinations of some frictionally generated silicate melts: Implications for fault zone rheology at high strain rates*, J. Geophys. Res. *98*, 8053–8068.

SPRAY, J. (1995), *Pseudotachylyte controversy; fact or friction?* Geology *23*, 1119–1122.

SPUDICH, P. and GUATTERI, M. (2004), *The effect of bandwidth limitations on the inference of earthquake slip–weakening distance from seismograms*, Bull. Sesim. Soc. Am. *94*, 6, 2028–2036.

SUPPE, J. *Principles of Structural Geology* (Prentice–Hall, Englewood Cliffs, N. J. 1985) 537 pp.

SUZUKI, T. and YAMASHITA, T. (2007), *Understanding of slip–weakening and –strengthening in a single framework of modeling and its seismological implications*, Geophys. Res. Lett. *34*, L13303, doi: 10.1029/2007GL030260.

TANIMOTO, T. and SHELDRAKE, K. P. (2002), *Three–dimensional S–wave velocity structure in Southern California*, Geophys. Res. Lett. *29*, 8, 1223, doi:10.1029/2001GL013486.

TCHALENKO, J. S. (1970), *Similarities between shear zones of different magnitudes*, Bull. Geol. Soc. Am. *81*, 1625–1640.

TEMPLETON, E. L. and RICE, J. R. (2008), *Off–fault plasticity and earthquake rupture dynamics: 1. Dry materials or neglect of fluid pressure changes*, J. Geophys. Res. *113*, B09306, doi: 10.1029/2007JB005529.

TERZAGHI, K., PECK, R. B., and MESRI, G. Soil Mechanics in Engineering Practice, 3rd ed. (John Wiley, Hoboken, N. J. 1996).

TINTI, E., BIZZARRI, A., PIATANESI, A., and COCCO, M. (2004), *Estimates of slip weakening distance for different dynamic rupture models*, Geophys. Res. Lett. *31*, L02611, doi: 10.1029/2003GL018811.

TSUTSUMI, A. and SHIMAMOTO, T. (1997), *High–velocity frictional properties of gabbro*, Geophys. Res. Lett. *24*, pp.699–702.

TULLIS, T. E. and Goldsby, D. L. (2003), *Flash melting of crustal rocks at almost seismic slip rates,* EOS Trans. AGU *84*, 46, Fall Meet. Suppl., Abstract S51B–05.

TULLIS, T. E. and WEEKS, J. D. (1986), *Constitutive behavior and stability of frictional sliding of granite*, Pure Appl. Geophys. *124*, 3, 383-414.

TURCOTTE, D. L. and SCHUBERT, G. *Geodynamics* (John Wiley and Sons, New York, USA. 1982).

VERMILYE, J. M. and SCHOLZ, C. H. (1988), *The process zone: A microstructural view of fault growth*, J. Geophys. Res. *103*, 12,223–12,237.

YAMASHITA, T. (2000), *Generation of microcracks by dynamic shear rupture and its effects on rupture growth and elastic wave radiation*, Geophys. J. Int. *143*, 395– 406.

WEERTMAN, J. (1980), *Unstable slippage across a fault that separates elastic media of different elastic constants*, J. Geophys. Res. *85*, B3, 1455-1461.

Wibberley, C. A. J. (2002), *Hydraulic diffusivity of fault gauge zones and implications for thermal pressurization during seismic slip*, Earth Planets Space, *54* (11), 1153–1171.

Wibberley, C. A. J. and Shimamoto, T. (2005), *Earthquake slip-weakening and asperities explained by thermal pressurization*, Nature *436* (4), 689–792, doi: 10.1038/nature03901.

Wilson, J. E., Chester, J. S., and Chester, F. M. (2003), *Microfracture analysis of fault growth and wear processes, Punchbowl Fault, San Andreas system, California*, J. Struct. Geol. *25*, 1855–1873.

(Received March 27, 2008, revised October 3, 2008, accepted March 2, 2009)
Published Online First: May 23, 2009